Published online 10 August 2019 *Nucleic Acids Research, 2019, Vol. 47, No. 17* **9087–9103**
doi: 10.1093/nar/gkz635

DREAM and RB cooperate to induce gene repression and cell-cycle arrest in response to p53 activation

Sigrid Uxa[1], Stephan H. Bernhart[2], Christina F. S. Mages[1], Martin Fischer[3], Robin Kohler[1], Steve Hoffmann[3], Peter F. Stadler[2,4,5,6,7,8], Kurt Engeland[1] and Gerd A. Müller[1,9,*]

[1]Molecular Oncology, Department of Gynaecology, Medical School, Leipzig University, 04103 Leipzig, Germany, [2]Transcriptome Bioinformatics Group, Department of Computer Science and Interdisciplinary Center for Bioinformatics, Leipzig University, 04107 Leipzig, Germany, [3]Computational Biology Group, Leibniz Institute on Aging – Fritz Lipmann Institute (FLI), 07745 Jena, Germany, [4]German Centre for Integrative Biodiversity Research (iDiv) Halle-Jena-Leipzig; Leipzig Research Center for Civilization Diseases; and Competence Center for Scalable Data Services and Solutions Dresden/Leipzig, Leipzig University, 04107 Leipzig, Germany, [5]Max Planck Institute for Mathematics in the Sciences, 04103 Leipzig, Germany, [6]Institute for Theoretical Chemistry, University of Vienna, A-1090 Wien, Austria, [7]Facultad de Ciencias, Universidad National de Colombia, Sede Bogota, Colombia, [8]Santa Fe Institute, Santa Fe, NM 87501, USA and [9]Department of Chemistry and Biochemistry, University of California, Santa Cruz, CA 95064, USA

Received April 11, 2019; Revised July 07, 2019; Editorial Decision July 09, 2019; Accepted July 16, 2019

ABSTRACT

Most human cancers acquire mutations causing defects in the p53 signaling pathway. The tumor suppressor p53 becomes activated in response to genotoxic stress and is essential for arresting the cell cycle to facilitate DNA repair or to initiate apoptosis. p53-induced cell cycle-arrest is mediated by expression of the CDK inhibitor p21$^{WAF1/Cip1}$, which prevents phosphorylation and inactivation of the pocket proteins RB, p130, and p107. In a hypophosphorylated state, pocket proteins bind to E2F factors forming RB-E2F and DREAM transcriptional repressor complexes. Here, we analyze the influence of RB and DREAM on p53-induced gene repression and cell-cycle arrest. We show that abrogation of DREAM function by knockout of the DREAM component LIN37 results in a reduced repression of cell-cycle genes. We identify the genes repressed by the p53-DREAM pathway and describe a set of genes that is downregulated by p53 independent of LIN37/DREAM. Most strikingly, p53-dependent repression of cell-cycle genes is completely abrogated in *LIN37*$^{-/-}$*;RB*$^{-/-}$ cells leading to a loss of the G_1/S checkpoint. Taken together, we show that DREAM and RB are key factors in the p53 signaling pathway to downregulate a large number of cell-cycle genes and to arrest the cell cycle at the G_1/S transition.

INTRODUCTION

An important function of the tumor suppressor p53 is to arrest the cell cycle in response to genotoxic stress (1). One mechanism to induce cell-cycle arrest is to prevent expression of proteins that are essential for progression through S phase and mitosis. Indeed, stabilization and post-translational activation of p53 increases the expression of several hundred target genes, but also leads to the downregulation of a similar number of genes. Many of the downregulated genes encode for important cell-cycle regulators such as cyclins, kinases, proteases, transcription factors, helicases, kinetochore components, DNA repair enzymes, etc. (2–5). The mechanisms of p53-dependent gene regulation have been discussed controversially, because it has long remained unclear how p53 can act as an activator but also as a repressor of transcription. However, recent experimental studies as well as meta-analyses provided evidence that p53-dependent gene repression is achieved through an indirect mechanism without binding of p53 to the repressed genes (2,6–8).

The indirect repression of cell-cycle genes by p53 includes activation of the *CDKN1A* gene encoding for the CDK inhibitor p21$^{WAF1/Cip1}$. p21 is a potent inhibitor of the cyclin-dependent kinases CDK4/6, CDK2 and CDK1 (9–11). Activity of these kinases is essential for phosphorylating the pocket proteins RB/p105, RBL1/p107 and RBL2/p130 (9,12–15). In their hypophosphorylated form, these proteins interact with members of the E2F transcription factor family to form transcriptional repressor complexes. While the retinoblastoma protein RB mainly binds to E2F1-3, p130 and p107 preferentially interact with E2F4 or E2F5

*To whom correspondence should be addressed. Tel: +49 341 9723637; Fax: +49 341 9723475; Email: gerd.mueller@medizin.uni-leipzig.de

© The Author(s) 2019. Published by Oxford University Press on behalf of Nucleic Acids Research.
This is an Open Access article distributed under the terms of the Creative Commons Attribution Non-Commercial License (http://creativecommons.org/licenses/by-nc/4.0/), which permits non-commercial re-use, distribution, and reproduction in any medium, provided the original work is properly cited. For commercial re-use, please contact journals.permissions@oup.com

as components of the DREAM complex. DREAM consists of p130 or p107 together with E2F4/DP or E2F5/DP and the MuvB core complex which is composed of LIN9, LIN54, LIN52, LIN37 and RBBP4 (16–23). Pocket proteins that have been phosphorylated by cyclin-CDK complexes dissociate from DREAM and RB-E2F repressor complexes. Subsequently, activator complexes are formed that stimulate transcription of genes essential for G_1/S and G_2/M transition (24,25). Thus, CDK inhibition through p53-mediated induction of p21 leads to hypophosphorylation of pocket proteins followed by accumulation and binding of DREAM and RB-E2F repressor complexes to cell-cycle gene promoters (3,4).

The DREAM complex binds to E2F elements in the promoters of G_1/S genes, but also to CHR promoter sites in G_2/M genes. In contrast, RB-E2F complexes can only interact with E2F sites. Thus, there is a set of genes bound by DREAM or RB-E2F and a separate set that is only bound by DREAM through CHR elements (20,25–28).

So far, hundreds of potential DREAM target genes have been identified. However, microarray analyses of RNA from p130/p107-null mouse embryonal fibroblasts yielded only 37 genes that showed an at least two-fold loss of repression in comparison to wild-type cells upon p53 induction (29). This is especially surprising since loss of p130/p107-binding to DREAM leads to deactivation of the entire complex (30,31). Furthermore, transcriptome analyses identifying p53-DREAM target genes in human cells are not available. It also remains unclear whether DREAM and RB cooperate to mediate p53-dependent gene repression.

We have recently shown that Lin37, a component of the MuvB core complex, is essential for DREAM repressor function and downregulation of cell-cycle genes in mouse cells in response to growth-restricting conditions (32). Interestingly, MuvB-dependent transcriptional activation is not perturbed in *Lin37*$^{-/-}$ cells. Moreover, the ability of these cells to exit the cell cycle and to enter quiescence is largely undisturbed. Similar observations were made in *Rb*$^{-/-}$ fibroblasts. In contrast, *Lin37*$^{-/-}$;*Rb*$^{-/-}$ NIH3T3 cells lost their potential to arrest in G_0/G_1 (32). Thus, *Lin37*$^{-/-}$ cells mirror the phenotype of *p107*$^{-/-}$;*p130*$^{-/-}$ cells and *Lin37*$^{-/-}$;*Rb*$^{-/-}$ cells phenocopy Rb, p107 and p130 triple knockouts (33–36).

Here, we combine LIN37 knockout in HCT116 colon carcinoma cells with knockout of RB to dissect the role of DREAM and RB in mediating p53-dependent downregulation of cell-cycle genes and cell-cycle arrest.

MATERIAL AND METHODS

Cell culture and drug treatment

HCT116 (37) and C2C12 (DSMZ) wild-type and knockout cells were grown in Dulbecco's modified Eagle's medium (Lonza) supplemented with 10 % fetal calf serum (Biochrom) and penicillin/streptomycin (Sigma-Aldrich) and maintained at 37° C and 10 % CO_2. Cells were tested negative for mycoplasma contamination by PCR with a mixture of primers that have been described earlier (38). Cells containing pRTS episomal plasmids were selected with Hygromycin B (Sigma-Aldrich) at a concentration of 200 mg/ml. Expression Lin37 or luciferase together with GFP was induced with doxycycline (Sigma-Aldrich) at a concentration of 500 ng/ml. Induced cells expressing GFP were isolated by flow cytometry sorting. For induction of p53, cells were treated with Nutlin-3a (10 μM; Cayman Chemicals) or doxorubicin (0.2 μg/ml; Medac GmbH) for 24 or 48 h.

Plasmids

Plasmids for the expression of Lin37 (32) and pGL4 luciferase reporter constructs were described earlier (26).

Generation of *LIN37*$^{-/-}$, *RB*$^{-/-}$ and *LIN37*$^{-/-}$;*RB*$^{-/-}$ HCT116 cell lines by CRISPR/Cas9 nickase

LIN37$^{-/-}$, *RB*$^{-/-}$ and *LIN37*$^{-/-}$;*RB*$^{-/-}$ HCT116 cells were created by CRISPR/Cas9 nickase applying the pX335-U6-Chimeric_BB-CBh-hSpCas9n(D10A) vector (39,40) as described earlier (32). InDel mutations were introduced in exon 6 of the LIN37 gene encoding for the LIN37-MuvB complex interaction domain (32) and in exon 13 of the RB gene encoding for the pocket domain which is essential for the interaction with E2F proteins (19). Sequences of the oligonucleotides are provided in Supplementary Table S1.

DNA affinity purifications

DNA affinity purifications of proteins from nuclear extracts of HCT116 *LIN37*$^{+/+}$ or *LIN37*$^{-/-}$ cells were performed and detected by western blot as described earlier (27).

SDS-PAGE and western blot

SDS-PAGE and western blot were performed following standard protocols as described earlier (41). The following antibodies were applied for protein detection: RB (C-2, Santa Cruz Biotechnology), LIN54 (A303-799A, Bethyl Laboratories), LIN9 (ab62329, Abcam), β-Actin (A5441, Sigma-Aldrich), RBBP4 (A301-206A, Bethyl Laboratories), LIN37 (custom-made at Pineda Antikörper-Service, Berlin, Germany) (26), p107 (C-18, sc-318, Santa Cruz Biotechnology), p130 (RBL2 D9T7M, Cell Signaling Technologies), FOXM1 (D12D5, Cell Signaling Technologies,) Aurora Kinase A (A300-071A, Bethyl Laboratories), cyclin B2 (A-2, sc-28303, Santa Cruz Biotechnology), KIF23 (MKLP-1, sc-136473, Santa Cruz Biotechnology), CDC25C (H-6, sc-13138, Santa Cruz Biotechnology), CDC6 (180.2, sc-9964, Santa Cruz Biotechnology), NEK2 (D-8, sc-55601, Santa Cruz Biotechnology), CCNE2 (EP454Y, ab40890, Abcam), p18 (118.2, sc-9965, Santa Cruz Biotechnology), PEG10 (4C10A7, Novus Biologicals), Survivin (71G4B7, Cell Signaling Technologies), p53 (Ab-6 DO-1, Merck/Calbiochem), p21 (Ab-1 EA10, Merck/Calbiochem), Histone H3 (1B1-B2, 61475, Active Motif). The monoclonal B-Myb LX015.1 antibody (hybridoma media 1:5) was a kind gift from Roger Watson (42).

RNA extraction, reverse transcription and semi-quantitative real-time PCR

Total RNA was isolated using TRIzol reagent (Invitrogen) following the manufacturer's protocol. One-step reverse transcription and quantitative real-time PCR were performed with an ABI 7300 Real-Time PCR System (Applied Biosystems) using the QuantiTect SYBR Green PCR Kit (Qiagen). See Supplementary Table S1 for primer sequences.

Next generation sequencing and transcriptome analysis

Cells were treated with Nutlin-3a (10 μM; Cayman Chemicals) for 48 h. Afterward cells were collected, and total RNA was extracted with the RNeasy Mini Kit (Qiagen).

RNA samples were sequenced using Illumina's next-generation sequencing methodology (43). In detail, quality check and quantification of total RNA was performed using the Agilent Bioanalyzer 2100 in combination with the RNA 6000 Nano Kit (Agilent Technologies). Libraries were constructed from 500 ng of total RNA using Illumina's TruSeq stranded mRNA Library Preparation Kit following the manufacturer's description.

Quantification and quality check of libraries were performed using the Agilent Bioanalyzer 2100 in combination with the DNA 7500 Kit. Libraries were pooled and sequenced in three lanes on a HiSeq2500 in 51cycle/single-end/high-output mode. Sequence information was extracted in FastQ format using Illumina's bcl2fastq v.1.8.4 resulting on average in 28.1 mio reads per sample.

RNA-Seq data generated for this publication was deposited at the European Nucleotide Archive as study PRJEB31044. Reads were trimmed with trimgalore (version 0.4.4, https://www.bioinformatics.babraham.ac.uk/projects/trim_galore/) using cutadapt version 1.8.3 (44) and fastqc v0.11.4 (http://www.bioinformatics.babraham.ac.uk/projects/fastqc) for quality control. About 30 % (29.2–30.2 %) of all reads contained adapter sequences that were trimmed. After trimming, a median of 0.1 % of all reads (maximum: 0.5 %) were too short to be considered mappable (<20 nt). The trimmed reads were mapped to the hg38 genome using segemehl (version 0.2.0 Rev: 417) (45), using standard parameters and the -S options to be able to map spliced reads. About 98 % (98.1 % to 98.8 %) of all reads were mapped by segemehl. Between 82.2 % and 84.7 % of all reads were mapped uniquely, and between 7.7 % and 9.1 % of the reads were spliced. The mapped genes were annotated using featureCounts (46) version 1.5.2 against the gencode v.27 annotation, using the following parameters: -O, -M, –fraction, -s 2, -t exon. We could annotate between 74.98 % and 79.62 % of all reads. The resulting gene counts were analyzed using DESeq2 (47) to find differentially expressed genes. RPK values computed from the featureCounts results were used for heatmap generation and fold change computation. Statistics of the sequencing are provided in Supplementary Table S4. Heatmaps were generated with Rs heatmap.2 function of the gplots package. Venn diagrams were built with R's VennDiagram package. GO term enrichments were computed using the DAVID (48) web-based analysis tool with all human genes as background.

Luciferase assays

Promoter activities were analyzed by luciferase reporter assays with extracts of transfected Nutlin-3a-treated HCT116 or C2C12 cells as described before (27). HCT116 (25,000 cells per well) and C2C12 (10,000 cells per well) were plated and transfected with 1 μl GeneJuice (EMD Millipore), 100 ng of promoter reporter plasmids (26) along with 200 ng of constructs expressing LIN37 (32) and 25 ng *renilla* luciferase plasmid (pGL4.70). Twenty four hours after transfection, cells were treated with Nutlin-3a (10 μM; Cayman Chemicals) for additional 24 h. Afterwards cells were lysed, and luciferase activity was measured with the Dual-Luciferase Reporter Assay system (Promega) following the manufacturer's recommendations. Luciferase relative light units were calculated by normalizing *firefly* luciferase activity to *renilla* luciferase activity.

Flow cytometry and cell sorting

The DNA content of HCT116 and C2C12 cells was analyzed by staining with propidium iodide (PI) followed by flow cytometry (LSR II, BC) as described earlier (27). Data was analyzed and figures were created with FlowJo (BD). Cells expressing GFP from pRTS episomes were isolated with a BD FACSAria II cell sorter.

EdU assay

EdU assays were performed with the Click-iT® EdU Flow Cytometry Assay Kits (ThermoFisher Scientific) according to manufacturer's information. 10,000 cells of each sample were analyzed by flow cytometry (LSR II, BC). Data was analyzed and figures were created with FlowJo (BD).

RESULTS

The DREAM component LIN37 is required for p53-dependent downregulation of cell-cycle genes

The HCT116 human colon carcinoma cell line is a standard tool to investigate p53 function (37). To analyze the role of DREAM-dependent transcriptional repression in p53 signaling, we created *LIN37*$^{-/-}$ HCT116 cells. Modified cell lines were expanded from single cell clones and analyzed for LIN37 expression. In several putative knockout clones, we still observed weak protein bands migrating with the same mobility as LIN37 (Figure 1A). These bands were not detected after MuvB complex purification with a MuvB-binding DNA probe revealing that the signal in the knockout cells is derived from a non-LIN37 protein (Figure 1A, E). Furthermore, mutations in *LIN37*$^{-/-}$ HCT116 clones were confirmed by DNA and RNA sequencing (data not shown).

Several of the resulting *LIN37*$^{-/-}$ HCT116 clonal cell lines were treated with the MDM2 inhibitor Nutlin-3a for 24 or 48 h, which led to accumulation of p53. To avoid clonal bias, we compared four independent *LIN37*$^{-/-}$ lines expanded from individual cells with the HCT116

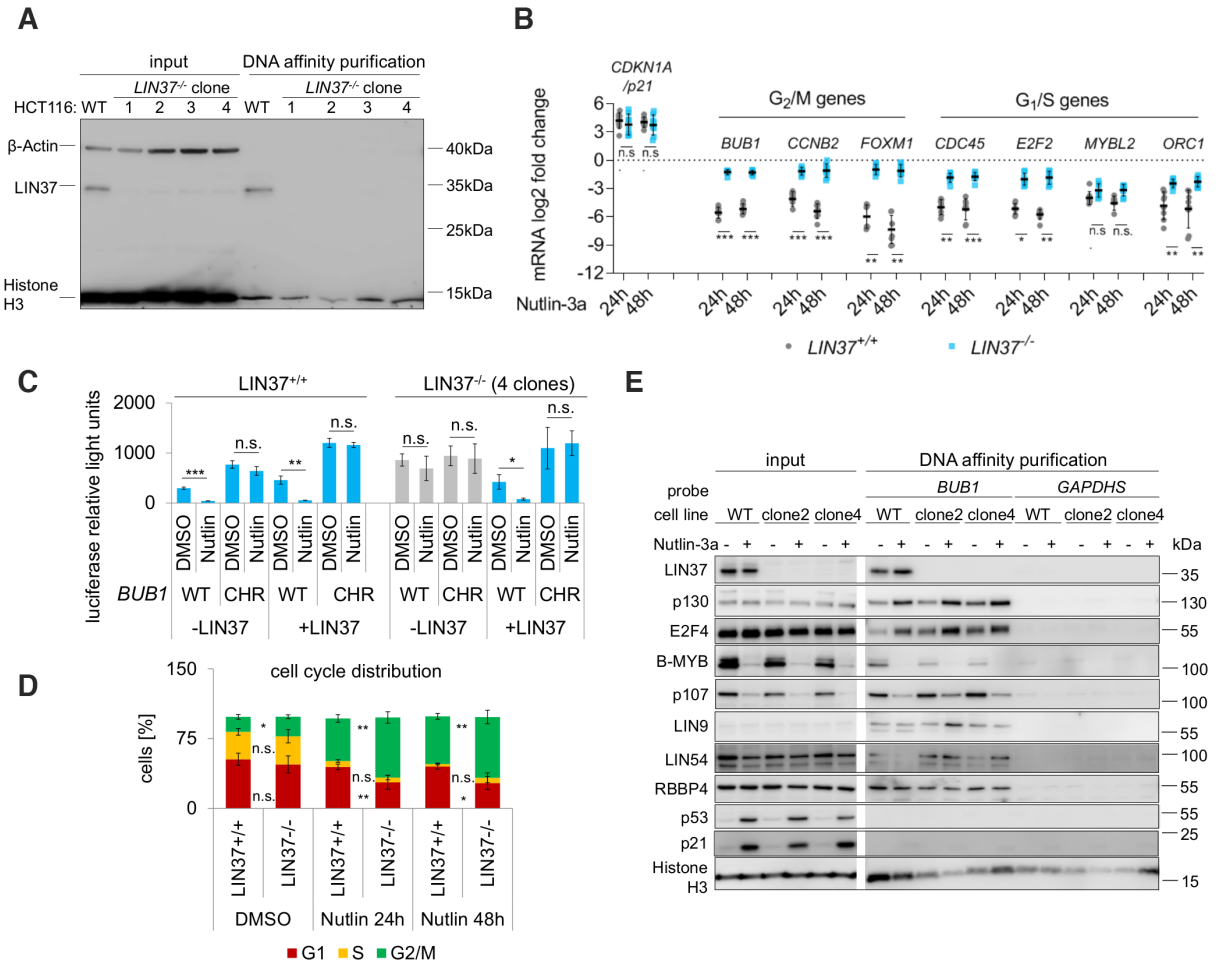

Figure 1. Loss of LIN37 impairs p53-dependent cell-cycle gene repression and G_1/S arrest. (**A**) Nuclear extracts prepared from HCT116 wild-type cells (WT) and four putative *LIN37* knockout (*LIN37*$^{-/-}$) clonal HCT116 cell lines were analyzed for LIN37 protein expression (input). In addition, MuvB complex components were purified with a *BUB1* promoter probe (DNA affinity purification). The non-DNA-binding protein β-Actin was analyzed to control the specificity of the purification, while histone H3 was probed to prove similar purification efficiencies. (**B**) HCT116 *LIN37*$^{+/+}$ ($n = 4$) and HCT116 *LIN37*$^{-/-}$ clonal cell lines (n = 4) were treated with Nutlin-3a for 24 or 48 h. Control cells were treated with DMSO for 48 h. mRNA expression of *CDKN1A/p21*, G_2/M-specific, and G_1/S phase genes was analyzed by RT-qPCR. The log2 fold changes of mRNA expression of treated versus control cells are given. Mean values are indicated by black bars. (**C**) The parental *LIN37*$^{+/+}$ HCT116 cell line or *LIN37*$^{-/-}$ clonal cell lines ($n = 4$) were transfected with *BUB1* wild-type (WT) or DREAM-binding site-deficient (CHR) promoter firefly luciferase reporter constructs together with a LIN37 expression plasmid (+LIN37) or an empty vector control (-LIN37). Promoters were tested for their activity upon treatment with DMSO (solvent control) or Nutlin-3a for 48 h. Promoter activities were normalized to *renilla* luciferase activity. Mean values ±SD of three biological replicates measured in one wild-type cell line or four *LIN37*$^{-/-}$ cell lines are given. (**D**) MuvB complex components were purified from nuclear extracts of the HCT116 parental cell line (WT) and from two independent *LIN37*$^{-/-}$lines (clone 2, clone 4) after treatment with Nutlin-3a or DMSO (neg. control) for 24 h. Purification was performed with a fragment of the *BUB1* promoter containing a CHR element or with a fragment of the *GAPDHS* promoter lacking DREAM binding sites to control for background binding. Protein binding of MuvB complex components was analyzed by western blotting. Expression of p53 and p21 was analyzed to control stabilization of p53 upon Nutlin-3a treatment, and histone H3 was probed as a control for DNA affinity purification. One representative experiment is shown. (**E**) Cell-cycle distribution of the *LIN37*$^{+/+}$ and *LIN37*$^{-/-}$ cell lines analyzed in (A) was measured after propidium iodide staining by flow cytometry. Mean values ±SD of wild-type and LIN37 knockout cell lines (n = 4) are given. Significances in (B), (C) and (E) were calculated with the Student's *t*-Test (n.s. – not significant, $^{*}P \leq .05$, $^{**}P \leq .01$, $^{***}P \leq .001$).

parental cell line and three clones that were identified as *LIN37*$^{+/+}$ after being subjected to the CRISPR/Cas9n procedure. *CDKN1A/p21* was equally activated in *LIN37*$^{+/+}$ and *LIN37*$^{-/-}$ cells after treatment with Nutlin-3a. Importantly, repression of G_2/M cell-cycle genes was significantly impaired in the knockout cells (Figure 1B): *LIN37*$^{+/+}$ cells responded to p53 activation by a 16- to 108-fold reduction of *BUB1*, *FOXM1* and *CCNB2* mRNA levels, but only a 2- to 2.5-fold repression remained in *LIN37*$^{-/-}$ cells. p53-dependent downregulation of G_1/S cell-cycle genes was also impaired in LIN37 knockout cells, although not as pronounced as observed for G_2/M genes. While the differences in mRNA levels of *ORC1*, *E2F2* and *CDC45* between *LIN37*$^{+/+}$ and *LIN37*$^{-/-}$ cells following Nutlin-3a treatment were significant, repression of the *MYBL2/B-MYB* gene was not significantly altered (Figure 1B).

Next, we re-expressed LIN37 in the four *LIN37*$^{-/-}$ clonal cell lines and analyzed the transcriptional activity of a *BUB1* promoter luciferase reporter construct (Figure 1C). The activity of the *BUB1* promoter was significantly repressed in the parental HCT116 cells when p53 was activated by Nutlin-3a. Mutation of the DREAM-binding CHR promoter element resulted in a complete loss of p53-dependent repression (Figure 1C). Overexpression of LIN37 in *LIN37*$^{+/+}$ cells did not affect repression of the wild-type promoter. In contrast, the *BUB1* promoter was not repressed in *LIN37*$^{-/-}$ cells. Mutation of the CHR did not have additional effects, indicating that loss of LIN37 completely abolishes DREAM repressor function. Importantly, re-expression of LIN37 rescued the gene repression defects observed in knockout cells. Taken together, the data suggest that p53-dependent repression requires LIN37 and binding of DREAM to CHR promoter elements.

Based on the observation that p53-dependent gene repression requires the DREAM component LIN37, we asked whether binding of DREAM to cell-cycle gene promoters is disturbed in *LIN37*$^{-/-}$ HCT116 cells. To test this, we purified MuvB complexes with a *BUB1* promoter probe from extracts of the parental HCT116 and from two *LIN37*$^{-/-}$ cell lines that were treated with DMSO (solvent control) or Nutlin-3a (Figure 1D). MuvB complex components were purified with similar efficiencies from *LIN37*$^{+/+}$ and *LIN37*$^{-/-}$ extracts. Binding of DREAM-specific proteins E2F4 and p130 to the DNA probe increased upon activation of p53, while total protein abundance remained unchanged. In contrast, protein levels of the G_1/S-specific proteins B-MYB and p107 were reduced in nuclear extracts of Nutlin-treated cells. Binding of B-MYB to the DNA probe was essentially lost following Nutlin-3a treatment. Protein levels of p53 and p21 increased after treating cells with Nutlin-3a. However, neither p53 nor p21 copurified with DREAM (Figure 1D). These observations show that DREAM can form and bind to DNA after p53 induction even when LIN37 is not present in the complex. Furthermore, p53 and p21, although at high concentrations in the cell, do not appear to associate with DREAM target promoters.

Loss of LIN37 impairs p53-dependent G_1/S cell-cycle arrest

We also analyzed the effect of LIN37 deletion on p53-mediated cell-cycle arrest. To this end, we compared the same four wild-type and *LIN37*$^{-/-}$ HCT116 clones that were tested for p53-dependent gene expression. Flow cytometry analyses revealed only minor differences in the cell-cycle distribution of DMSO-treated *LIN37*$^{+/+}$ and *LIN37*$^{-/-}$ cells (Figure 1E). As expected, treatment of *LIN37*$^{+/+}$ cells with Nutlin-3a for 24 or 48 h led to a decrease of S phase cells compared to DMSO solvent control-treated cells (8,49) suggesting an activation of the G_1 and G_2 checkpoints. While Nutlin-3a treatment led to a similar depletion of the S phase population in *LIN37*$^{-/-}$ cells, the fraction of G_1 cells was significantly decreased in comparison to wild-type cells, while the G_2/M population increased (Figure 1E). These findings indicate that the G_1/S checkpoint induced by Nutlin-3a through p53 is compromised in *LIN37*$^{-/-}$ cells.

Lin37 is essential for p53-dependent cell-cycle gene repression in mouse C2C12 cells

Next, we tested whether the findings from human cells are also observed in a mouse cell line. To this end, *Lin37*$^{-/-}$ C2C12 cells were employed that we had generated earlier (32). We analyzed four wild-type and four *Lin37*$^{-/-}$ clonal cell lines (Figure 2). qPCR analyses revealed that *Cdkn1a/p21* mRNA expression was elevated upon Nutlin-3a treatment in wild-type and mutant cells (Figure 2A). Expression of mRNA from G_1/S and G_2/M cell-cycle genes was downregulated in wild-type cells. While the repression of the G_2/M genes *Bub1*, *Foxm1* and *Cdc25c* was substantially impaired in *Lin37*$^{-/-}$ cells, the G_1/S genes *E2f2* and *Mybl2* were still partially repressed upon Nutlin-3a treatment even in the absence of Lin37 (Figure 2A). Nutlin-3a treatment led to an accumulation of G_1 and G_2 cells and to a reduction of the S phase population in both *Lin37*$^{+/+}$ and *Lin37*$^{-/-}$ cells. In contrast to HCT116 cells, more cells accumulated in G_1 than in G_2. However, fewer cells arrested in G_1 in a Lin37-negative background which suggests an attenuation of the G_1 checkpoint (Figure 2B). Furthermore, re-expression of Lin37 in the *Lin37*$^{-/-}$ C2C12 cells restored repression of the *Ttk* and *Orc1* promoters in luciferase reporter assays (Figure 2C). The results generated in the mouse system are largely in line with the data generated with the human cells. These observations suggest that the role of the DREAM component LIN37 to mediate p53-dependent cell-cycle arrest and downregulation of cell-cycle genes is evolutionarily conserved.

A genome-wide screen identified 268 genes repressed by the p53-DREAM pathway

To assess the influence of LIN37 on global p53-dependent gene expression, we performed RNA-seq of two distinct *LIN37*$^{-/-}$ HCT116 clonal cell lines stably transfected with episomal vectors expressing LIN37 and GFP or only GFP and determined the expression changes in knockout or LIN37 rescue cells upon Nutlin-3a treatment. We compared the ensuing data set with the results of a recent meta-analysis of p53-dependent gene regulation (2). We found a strong correlation of the mRNA expression changes (log2FC) in the LIN37-rescue cells upon Nutlin-3a treatment with p53 expression scores compiled from 20 data sets (see caption of Figure 3 for details) (Figure 3A). Genes substantially activated or repressed in our experiments were generally also identified as being up- or downregulated, respectively, in other genome-wide datasets as represented by a particular high or low p53 expression score. This strong correlation (Spearman rho 0.74) of our results with the meta-analysis supports the high quality of our data set.

In concordance with earlier results (2), our data also show that many genes are activated by p53 through direct binding as indicated by high p53 ChIP scores (Figure 3B) and genes repressed by p53 typically bind the DREAM complex (high DREAM component ChIP score, see caption of Figure 3 for details). The genes most substantially repressed exhibited also the highest ChIP scores for DREAM components (Figure 3C).

We identified 3342 differentially expressed genes ($P_{adj} \leq 0.001$) between DMSO- and Nutlin-treated LIN37 rescue

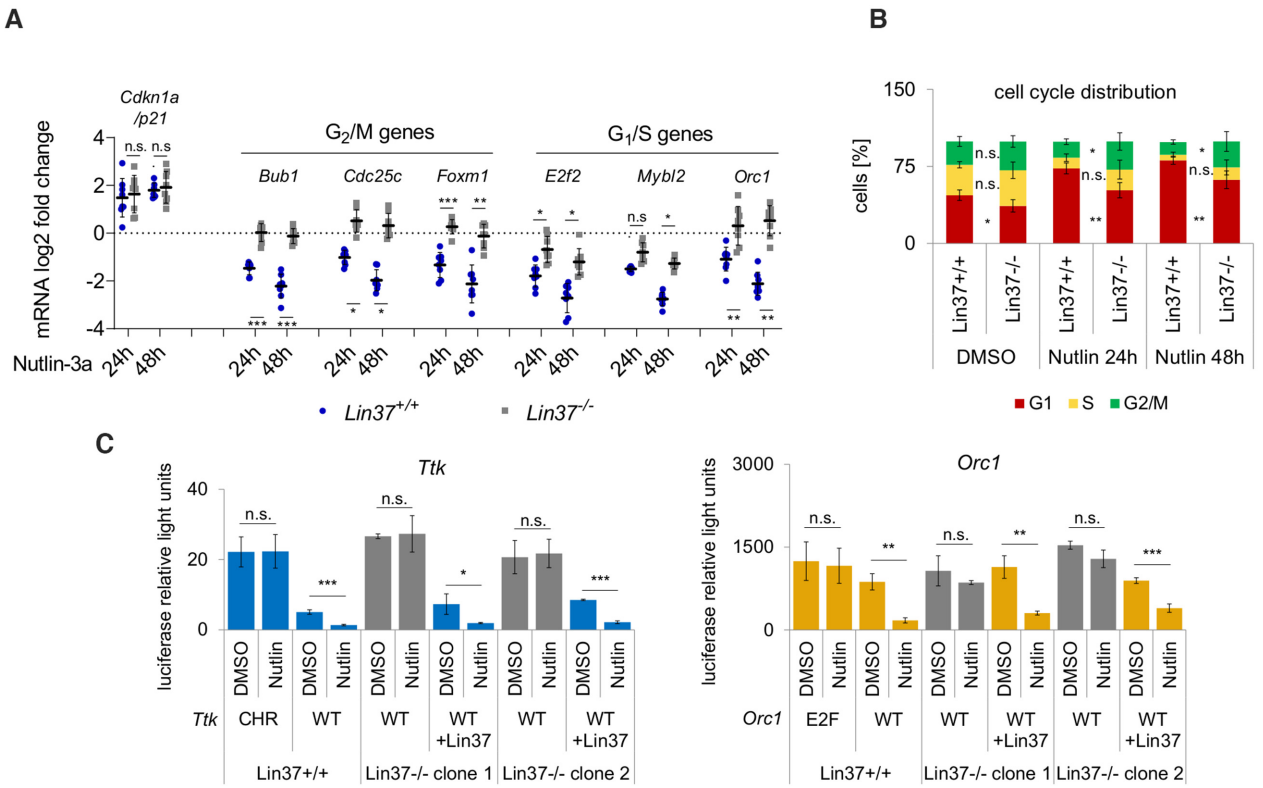

Figure 2. Loss of Lin37 impairs p53-dependent cell-cycle gene repression and G_1/S arrest in mouse C2C12 cells. (**A**) Wild-type C2C12 clonal cell lines (*LIN37*$^{+/+}$, $n = 4$) and mutant C2C12 *Lin37*$^{-/-}$ clonal cell lines ($n = 4$) were treated with Nutlin-3a for 24 or 48 h. Control cells were treated with DMSO for 48 h. mRNA expression of *CDKN1A/p21*, G_2/M-specific, and G_1/S phase genes was analyzed by RT-qPCR. The $\log_2$ fold changes of mRNA expression of treated vs. control cells are given. Mean values (black bars) of mRNA expression from four cell lines determined with two technical replicates are given. (**B**) Cell-cycle distribution of the *Lin37*$^{+/+}$ and *Lin37*$^{-/-}$ cell lines analyzed in (A) was measured after propidium iodide staining by flow cytometry. Mean values ±SD of wild-type (Lin37+/+, $n = 4$) and Lin37 knockout lines (Lin37–/–, $n = 4$) are shown. (**C**) The parental C2C12 cell line and the two *Lin37*$^{-/-}$ clonal cell lines were transfected with *Ttk* (blue) or *Orc1* (yellow) wild-type (WT) or DREAM-binding site-deficient (CHR, E2F sites) promoter firefly luciferase reporter constructs. The reporter plasmids were cotransfected with a Lin37-expression plasmid (+Lin37) or an empty vector (-Lin37). Promoter activities were determined upon treatment with DMSO (control) or Nutlin-3a for 24 h and normalized to *renilla* luciferase activity as a standard from a cotransfected plasmid. Mean values ±SD of three biological replicates are given. All significances were calculated with the Student's *t*-Test (n.s. – not significant, $^{*}P \leq .05$, $^{**}P \leq .01$, $^{***}P \leq .001$).

cells. Next, we calculated the differences between the expression changes (log2FC) upon Nutlin-3a treatment in LIN37 knockout and rescue cells (Δlog2FC). Thus, a reduced p53-dependent repression or an increased activation of a particular gene in *LIN37*$^{-/-}$ cells resulted in a negative Δlog2FC, while genes substantially repressed or weaker activated received a Δlog2FC >0. We then plotted the p53 $\log_2$FCs of rescue cells versus the Δlog2FCs (Figure 3D). These data showed that loss of LIN37 mainly affects regulation of genes that are repressed by p53 and that *LIN37*$^{-/-}$ cells have a reduced potential to downregulate genes through the p53 pathway. Furthermore, there was a strong correlation between the magnitude of p53 repression and LIN37 dependency: repression of genes that are considerably downregulated by p53 generally was dependent on LIN37/DREAM.

With a few exceptions, the top 100 p53-repressed genes exhibited a clearly attenuated p53-dependent gene downregulation in *LIN37*$^{-/-}$ cells (Figure 3E). Furthermore, over 85 % of p53-LIN37 target genes were identified as cell-cycle genes with a maximum expression in G_1/S or G_2/M phases. Also, these genes generally obtained a high DREAM ChIP score indicating that loss of LIN37 mainly has a negative effect on the repression of cell-cycle genes that intensely bind the DREAM complex. This was observed for G_1/S as well as for G_2/M genes. In contrast, binding of RB/E2F was mainly detected at genes with maximum expression in G_1/S which supports our finding that G_2/M genes are largely regulated by DREAM/MuvB, while G_1/S genes are regulated by both DREAM and RB-E2F complexes (26,28).

About 80% of the genes identified here as p53-LIN37 targets were also downregulated in a Lin37-dependent manner in quiescent NIH3T3 mouse fibroblasts (32) (Figure 3E). This substantial overlap supports the observation that downregulation of cell-cycle genes in response to both p53 activation and growth-limiting conditions employs the mammalian DREAM complex.

Among the 100 genes that were most substantially repressed by p53, only 7 did not show a reduced repression in *LIN37*$^{-/-}$ cells. These genes generally obtained low DREAM binding scores (Figure 3E). Interestingly, one of those genes is *CCNE2*, which appears on fifth position of the most substantially repressed p53 target genes in LIN37 rescue cells (log2FC = –4.42), and its repression is not im-

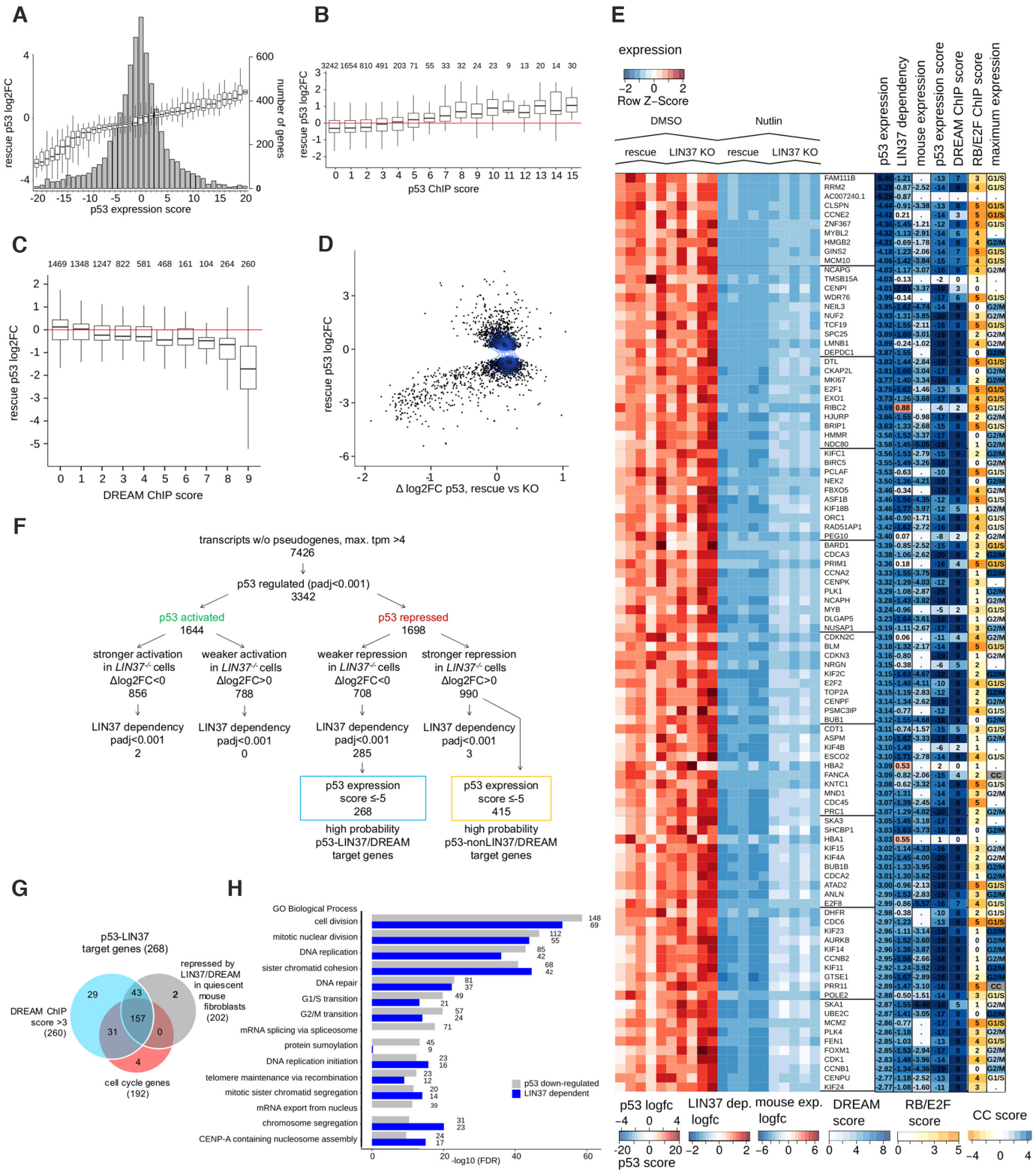

Figure 3. Identification of genes repressed by p53 in a LIN37/DREAM-dependent manner. (**A**) Box plots (left axis of ordinates): Expression alterations (log2-fold change) in LIN37 rescue cells upon Nutlin-3a treatment vs. p53 expression score compiled from 20 data sets of p53-dependent mRNA expression data. A score of -20 indicates significant repression of a specific gene in 20 data sets. A score of 0 shows that there is no p53-dependent activation and repression or that the sum of significant change from 20 data sets is balanced. A score of +20 indicates activation in all data sets (2). Barplots (right axis of ordinates) show the number of genes with the respective p53 expression score. (**B**) Expression changes (log2-fold change) in LIN37 rescue cells upon Nutlin-3a treatment vs. p53 ChIP score derived from 15 independent experiments. A score of 15 equals p53 binding to a specific gene detected in all experiments and a score of 0 equals no detectable p53 binding in any experiment (2). The number of genes with the respective ChIP score is shown above the box

paired in *LIN37*$^{-/-}$ cells ($\log_2$FC = –4.63, $\Delta\log_2$FC = 0.21).

To define a set of high probability p53-LIN37/DREAM target genes, we further analyzed genes regulated by p53 with high significance ($P_{adj} < 0.001$) in the rescue cells (Figure 3F). We asked how many of these genes showed highly significant differences in p53-dependent expression changes ($P_{adj} < 0.001$) between LIN37 knockout and rescue cells. This approach dramatically decreased the number of genes regulated in a p53- and LIN37-dependent manner. Only two out of the set of p53-activated genes showed a significant LIN37 dependency and were slightly stronger activated in the *LIN37*$^{-/-}$ cells (*TINAGL1*, *ACHE1*). In contrast, the vast majority of 288 genes downregulated by p53 significantly depend on LIN37. Out of these 288 genes, 285 exhibited a reduced p53-dependent repression, while only three genes (*LAMB1*, *ARMC4*, *KCNH3*) showed a stronger repression in the knockout cells (Figure 3F, Supplementary Table S2). These numbers support the conclusion drawn from the data shown in Figure 3D: Essentially only gene repression by p53 was disturbed upon loss of LIN37, while LIN37 knockout had hardly any effect on genes activated by p53.

Out of the 285 p53-LIN37-repressed genes, we selected the ones that obtained a *p53 expression score* ≤ –5 (2) to identify genes that are regulated by p53 across various cell types and are repressed after different treatments to induce p53. We obtained a final set of 268 genes which we designate as high probability p53-LIN37/DREAM target genes (Figure 3F, Table 1, Supplementary Table S2). Of these 268 genes, 260 had a DREAM ChIP score >3, 192 were shown to have a cell cycle-dependent mRNA expression with maximum expression in G_1/S or G_2/M (2), and 202 were also identified as Lin37/DREAM targets in mouse fibroblasts (32) (Figure 3G).

We then performed gene ontology (GO) analyses with the sets of p53-repressed genes and high probability p53-LIN37/DREAM target genes (Figure 3H, Supplementary Table S3). The top 15 most significantly enriched biological processes largely represented cell-cycle regulation. Interestingly, three GO terms were enriched in all p53-repressed genes with high significance, but not in p53-LIN37/DREAM-repressed genes: (I) mRNA splicing via spliceosome, (II) protein sumoylation, and (III) mRNA export from nucleus. Thus, most cell-cycle genes are repressed by p53 in a LIN37/DREAM-dependent manner and genes repressed by p53 independently of LIN37/DREAM are mostly not cell-cycle genes.

Taken together, these analyses show that LIN37/DREAM plays a central role in p53-dependent gene repression. The regulation of most genes substantially repressed by p53 depends on LIN37. However, considering that we identified 1698 genes significantly repressed by p53, there is also a large set of genes that is repressed by p53 independent of LIN37 (Figure 3F).

Combined knockout of RB and LIN37 leads to a complete deregulation of p53-dependent cell-cycle gene expression

Activation of the p53-p21 signaling pathway inhibits CDK activity which supports the formation of both DREAM and RB-containing complexes. Because of distinct and overlapping functions of these complexes, we asked how loss of the particular repressors alters cell-cycle gene expression and induction of cell-cycle arrest by p53. We generated *RB*$^{-/-}$ and *LIN37*$^{-/-}$;*RB*$^{-/-}$ HCT116 cells with a CRISPR/Cas9 nickase approach by targeting exon 13 of the RB gene, which partially encodes the pocket domain. Thus, even if truncated RB variants were expressed, they would not be able to interact with E2F proteins (50,51). Several *RB*$^{-/-}$ and *LIN37*$^{-/-}$;*RB*$^{-/-}$ cell lines were identified and compared with HCT116 wild-type and *LIN37*$^{-/-}$ cells.

First, we treated all cell lines with Nutlin-3a or, as an alternative way to activate p53, with doxorubicin. In wild-type cells, all analyzed cell-cycle genes showed substantial repression with both treatments. Nutlin-3a and doxorubicin had almost identical effects on gene expression in *LIN37*$^{-/-}$ cells. In these cells, repression of G_1/S and G_2/M genes was impaired with both treatments. These effects were more pronounced for G_2/M than for G_1/S genes. Especially for the *RBL1/p107* gene, the influence of LIN37 loss on the p53-dependent repression was only moderate. Treatment of the *RB*$^{-/-}$ cells with Nutlin-3a resulted in a large decrease of G_2/M gene expression (*BUB1*, *CCNB2*, *NEK2*) with only a minor loss of repression compared to wild-type cells. In contrast, downregulation of G_1/S genes (*ORC1*, *E2F2*, *RBL1/p107*) was almost completely lost (Figure 4A). Interestingly, treatment with doxorubicin led to nearly the same deregulation of G_1/S and G_2/M genes in *RB*$^{-/-}$ cells. Thus, the influence of RB on the repression of G_2/M genes clearly depends on the way of p53 activation. RB appears to be particularly important for the repression of G_2/M genes when p53 is activated by doxorubicin-mediated induction of

←

plots. (**C**) Expression changes (log2 fold change) in LIN37 rescue cells upon Nutlin-3a treatment vs. DREAM ChIP score derived from nine independent experiments. A score of 9 illustrates binding of DREAM components to a specific gene detected in all experiments and a score of 0 equals no detectable DREAM component binding in any experiment (2). The number of genes with the respective DREAM score is shown above the box plots. (**D**) Expression change (log2 fold change) upon Nutlin-3a treatment in LIN37 rescue cells vs. difference in expression change upon Nutlin-3a treatment between LIN37 knockout and rescue cells (Δlog2FC p53 rescue versus KO). (**E**) The 100 genes most substantially downregulated upon Nutlin-3a treatment in LIN37 rescue cells. Left: Expression heatmap (from left to right: DMSO treated LIN37 rescue cells, DMSO treated *LIN37*$^{-/-}$ cells, Nutlin-3a treated rescue cells, Nutlin-3a treated *LIN37*$^{-/-}$ cells (5 biological replicates each). Right: Color coded columns showing (left to right): log2 fold change of expression upon Nutlin-3a treatment, difference of log2 fold change after Nutlin-3a treatment between rescue and *LIN37*$^{-/-}$ cells, log2 fold change between serum-starved rescue and *LIN37*$^{-/-}$ mouse NIH3T3 fibroblasts (32), DREAM ChIP score, RB-E2F ChIP score, and the peak of expression if cell cycle-related (CC if cell cycle-dependent without clear preference for either G_1/S or G_2/M) (2). (**F**) Selection of gene sets based on the transcriptome analysis. The numbers correspond to the genes in the respective groups. (**G**) Venn diagram of genes downregulated upon Nutlin-3a treatment as defined in (F): Overlap of genes with DREAM ChIP score >3, genes repressed by LIN37/DREAM in serum-starved mouse fibroblast and established cell-cycle genes. (**H**) False discovery rate (FDR) of top 15 GO term (Gene Ontology Biological Process) enrichments of genes downregulated upon Nutlin-3a treatment. Grey: all downregulated genes, blue: LIN37-dependent downregulation. The respective number of genes is given to the right of the bars.

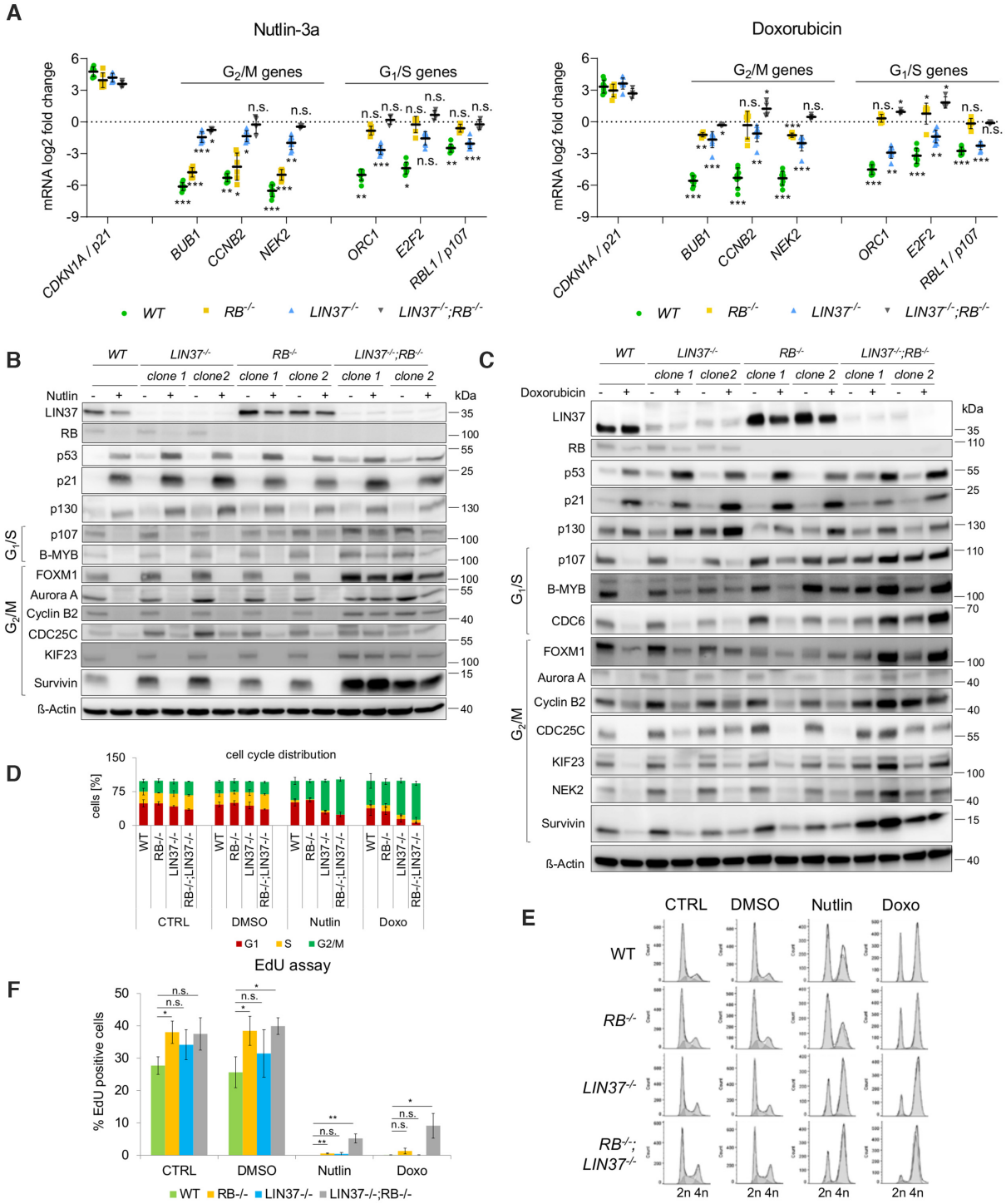

Figure 4. *LIN37*$^{-/-}$;*RB*$^{-/-}$ HCT116 cells lack the ability do downregulate cell-cycle gene expression on mRNA and protein levels in response to p53 activation and exhibit a compromised G_1/S checkpoint. (**A**) HCT116 wild-type (WT, $n = 4$), *RB*$^{-/-}$ ($n = 3$), *LIN37*−/− ($n = 4$), and *RB*$^{-/-}$;*LIN37*$^{-/-}$ ($n = 2$) clonal cell lines were treated with Nutlin-3a or doxorubicin for 48 h. As controls, untreated or DMSO-treated (48 h) cell lines were analyzed. mRNA expression of the CDK inhibitor *CDKN1A/p21*, G_2/M-specific genes, and G_1/S phase genes were measured by RT-qPCR. The log2 fold changes of mRNA expression of treated vs. control cells are given. Mean values are indicated by black bars. Protein expression of cell-cycle regulators in response to 48 h of (**B**) Nutlin-3a or (**C**) doxorubicin treatment in HCT116 wild-type (WT) and two clonal cell lines each of *RB*$^{-/-}$, *LIN37*$^{-/-}$, and *RB*$^{-/-}$;*LIN37*$^{-/-}$ HCT116 cells were analyzed by western blot. β-Actin served as a loading control. (**D**) Cell-cycle distribution of cell lines analyzed in (A) was measured by flow cytometry after propidium iodide staining. Mean values ±SD of wild-type (WT, $n = 4$) and knockout cell lines (RB−/− ($n = 3$), LIN37−/−, n = 4, RB−/−;LIN37−/− ($n = 2$)) are given (n.s. – not significant, $^{*}P \leq .05$, $^{**}P \leq .01$, $^{***}P \leq .001$). (**E**) One representative experiment is shown. (**F**) Amount of S phase cells in untreated (CTRL) or DMSO-, Nutlin-3a-; and doxorubicin- (Doxo) treated wild-type and knockout cells as determined by EdU incorporation assays with 3 biological replicates. Significance was calculated with the Student's *t*-Test (n.s. – not significant, $^{*}P \leq .05$, $^{**}P \leq .01$, $^{***}P \leq .001$).

Table 1. 268 genes repressed through the p53-LIN37/DREAM pathway

ACD	C16orf59/TEDC2	*CDK1*	*CEP72*	*DTL*	*FANCI*	*HMMR*	*KIFC1*	*MTBP*	*NUSAP1*	*PRC1*	*SCLT1*	*TK1*	*ZGRF1*
ANLN	*C18orf54/LAS2*	*CDT1*	*CEP78*	*DTYMK*	*FEN1*	*INCENP*	*KNL1*	*MTFR2*	*OIP5*	*PRIM2*	*SGO1*	*TONSL*	*ZNF107*
ARHGAP11A	*C1orf112*	*CENPA*	*CHAF1A*	*E2F1*	*FOXM1*	*INIP*	*KNSTRN*	*MYBL1*	*ORC1*	*PRR11*	*SGO2*	*TOP2A*	*ZNF367*
ARHGAP11B	*C4orf46/RCDG1*	*CENPE*	*CHEK1*	*E2F2*	*FOXRED1*	*IQGAP3*	*KNTC1*	*MYBL2*	*ORC3*	*PSMC3IP*	*SHCBP1*	*TOPBP1*	*ZNF695*
ARHGEF39	*C5orf34*	*CENPF*	*CHTF18*	*E2F8*	*G2E3*	*ITGB3BP*	*LIN9*	*NCAPD2*	*ORC6*	*PSRC1*	*SKA1*	*TPX2*	*ZNF714*
ASF1B	*CCDC150*	*CENPH*	*CIT*	*ECT2*	*GEN1*	*KCNK5*	*LRR1*	*NCAPD3*	*PARPBP*	*RACGAP1*	*SKA3*	*TRAIP*	*ZNF92*
ASPM	*CCDC18*	*CENPI*	*CKAP2L*	*EME1*	*GGH*	*KIAA1524*	*LSM5*	*NCAPG*	*PBK*	*RAD18*	*SLC25A10*	*TRIP13*	*ZWILCH*
ATAD2	*CCDC77*	*CENPJ*	*CKS2*	*ERCC6L*	*GINS1*	*KIF11*	*MAD2L1*	*NCAPG2*	*PIF1*	*RAD51*	*SMC2*	*TROAP*	*ZWINT*
ATAD5	*CCNA2*	*CENPK*	*DBF4B*	*ESCO2*	*GINS2*	*KIF14*	*MASTL*	*NCAPH*	*PIGK*	*RAD51AP1*	*SMC4*	*TTK*	
AUNIP	*CCNB1*	*CENPL*	*DCK*	*ESPL1*	*GINS4*	*KIF15*	*MCM10*	*NDC80*	*PIMREG*	*RAD54B*	*SPAG5*	*TUBD1*	
AURKA	*CCNB2*	*CENPM*	*DCLRE1B*	*EXO1*	*GMNN*	*KIF18A*	*MCM2*	*NEIL3*	*PKMYT1*	*RAD54L*	*SPC24*	*UBE2C*	
AURKB	*CDC20*	*CENPN*	*DDIAS*	*FAAP24*	*GPSM2*	*KIF18B*	*MCM3*	*NEK2*	*PLK1*	*RECQL4*	*SPC25*	*UBE2T*	
BIRC5	*CDC25A*	*CENPO*	*DDX11*	*FAM72A*	*GSTCD*	*KIF20A*	*MCM4*	*NEMP1*	*PLK4*	*RFC3*	*SPDL1*	*UNG*	
BLM	*CDC25C*	*CENPQ*	*DEPDC1*	*FAM72B*	*GTSE1*	*KIF20B*	*MCM5*	*NIF3L1*	*POC1A*	*RFC4*	*STIL*	*VRK1*	
BORA	*CDC45*	*CENPU*	*DEPDC1B*	*FAM72D*	*H2AFX*	*KIF22*	*MCM8*	*NMU*	*POLA1*	*RFC5*	*SUV39H1*	*WBP11*	
BRCA1	*CDC6*	*CENPW*	*DIAPH3*	*FAM83D*	*H2AFZ*	*KIF23*	*MELK*	*NSD2*	*POLA2*	*RHNO1*	*SUV39H2*	*WDR62*	
BRIP1	*CDCA2*	*CEP135*	*DLGAP5*	*FANCA*	*HASPIN*	*KIF24*	*MIS18A*	*NUDT1*	*POLD1*	*RNASEH2A*	*TACC3*	*WEE1*	
BUB1	*CDCA3*	*CEP152*	*DNA2*	*FANCB*	*HJURP*	*KIF2C*	*MIS18BP1*	*NUF2*	*POLE*	*RRM1*	*TCF19*	*XRCC1*	
BUB1B	*CDCA5*	*CEP295*	*DSCC1*	*FANCD2*	*HMGB1*	*KIF4A*	*MKI67*	*NUP107*	*POLQ*	*RTTN*	*TICRR*	*XRCC2*	
C14orf80/TEDC1	*CDCA8*	*CEP55*	*DSN1*	*FANCG*	*HMGB2*	*KIF4B*	*MND1*	*NUP93*	*PPIH*	*SASS6*	*TIMELESS*	*XRCC3*	

Genes were selected by the following criteria: (I) significantly repressed by p53 ($P_{adj} < 0.001$), (II) significantly deregulated in Nutlin-treated *LIN37*$^{-/-}$ cells ($P_{adj} < 0.001$), and (III) p53 expression score ≤ -5.

DNA damage. Importantly, all analyzed genes were completely deregulated in *LIN37*$^{-/-}$;*RB*$^{-/-}$ double knockout cells after both treatments (Figure 4A).

We then analyzed whether the observed changes in mRNA expression translate to the protein levels. Nutlin-3a (Figure 4B) and doxorubicin (Figure 4C) treatment led to an accumulation of p53 and p21 proteins in all cell lines. Consistent with earlier work (52) the level of p130 protein increased after p53 activation, while RB levels decreased upon Nutlin-3a or doxorubicin treatment in all cell types tested (Figure 4B and C).

Most analyzed cell-cycle proteins were similarly downregulated in *LIN37*$^{-/-}$ as well as in *RB*$^{-/-}$ single knockout cells. However, expression of the G_1/S protein p107 was reduced by Nutlin-3a and doxorubicin in wild-type and *LIN37*$^{-/-}$ cells, but we observed an obvious loss of repression in *RB*$^{-/-}$ cells. In contrast, downregulation of CDC25C, which is maximally expressed in G_2/M, was less pronounced in *LIN37*$^{-/-}$ cells. Repression of protein levels appeared to be generally lower in the doxorubicin-treated cells than following Nutlin-3a treatment, but loss of LIN37 and/or RB had similar consequences with both treatments. Most strikingly, repression of all cell-cycle proteins was completely lost in the *LIN37*$^{-/-}$;*RB*$^{-/-}$ double knockout cells (Figure 4B and C).

G_1/S arrest is compromised in LIN37/RB double knockout cells

Next, we analyzed whether the knockout cells differed in their ability to arrest in the cell cycle upon p53 activation. In all cell lines tested, the S phase fraction substantially decreased after treatment with Nutlin-3a or doxorubicin (Figure 4D). In wild-type cells, accumulation in fractions with 2n and 4n DNA content was observed reflecting both G_1/S and G_2/M arrests. While Nutlin-3a treatment led to an increase of both 2n and 4n cell populations, induction of DNA damage by doxorubicin resulted in a more pronounced accumulation of the 4*n* cell fraction. Interestingly, the ability to arrest in G_1 and G_2 appeared largely unperturbed in *RB*$^{-/-}$ cells. In contrast, the fraction of LIN37-deficient cells arresting in G_1 phase upon p53 induction was clearly diminished. In the double knockouts, this effect was even more pronounced resulting in an almost complete loss of the G_1 population in the doxorubicin treated cells (Figure 4D, E). Thus, combined loss of DREAM and RB function compromises the G_1/S checkpoint and leads to an accumulation of cells in G_2.

The automated analysis of DNA content by the FlowJo software did not yield a change in the S phase fraction in *LIN37*$^{-/-}$;*RB*$^{-/-}$ cells upon p53 activation in comparison to the other cell lines (Figure 4D). However, visual evaluation of the histograms indicated an increase in the number of S phase cells (Figure 4E). To analyze the S phase population with a more accurate approach, we performed EdU incorporation experiments. The acquired data showed that combined loss of LIN37 and RB led to a significant increase of S phase cells (Figure 4F). Thus, although most cells can still arrest in G_2 in the absence of LIN37 or RB, a substantial fraction of these cells can escape the arrest. Taken together, these observations suggest that *LIN37*$^{-/-}$;*RB*$^{-/-}$ cells show a substantially impaired arrest at the G_1/S checkpoint and also can progress through the G_2/M checkpoint.

Identification of genes repressed by p53 independent of LIN37/DREAM

In the transcriptome analysis, 1698 genes were significantly downregulated in response to treatment with Nutlin-3a ($P_{adj} < 0.001$). However, 990 of these genes did not show any impaired repression in *LIN37*$^{-/-}$ cells (Δlog2FC > 0) (Figure 3F, Supplementary Table S2). We sought to test whether downregulation of this gene set was mediated by RB or whether it was completely independent of pocket protein-containing complexes. To this end, we selected genes that were repressed by p53 across cell types and treatments (p53 repression score $\leq$ -5), but independent of LIN37 (n = 415) (Figure 3F, Table 2, Supplementary Table S2). These genes were generally less repressed by p53 in the LIN37 rescue cells than the set of p53-LIN37/DREAM target genes (medium log2FC LIN37-dependent genes = -2.28 versus LIN37-independent = -0.95). When we analyzed the top 100 of the 415 genes downregulated by p53 in a LIN37-independent manner (Figure 5A), only 12 genes were re-

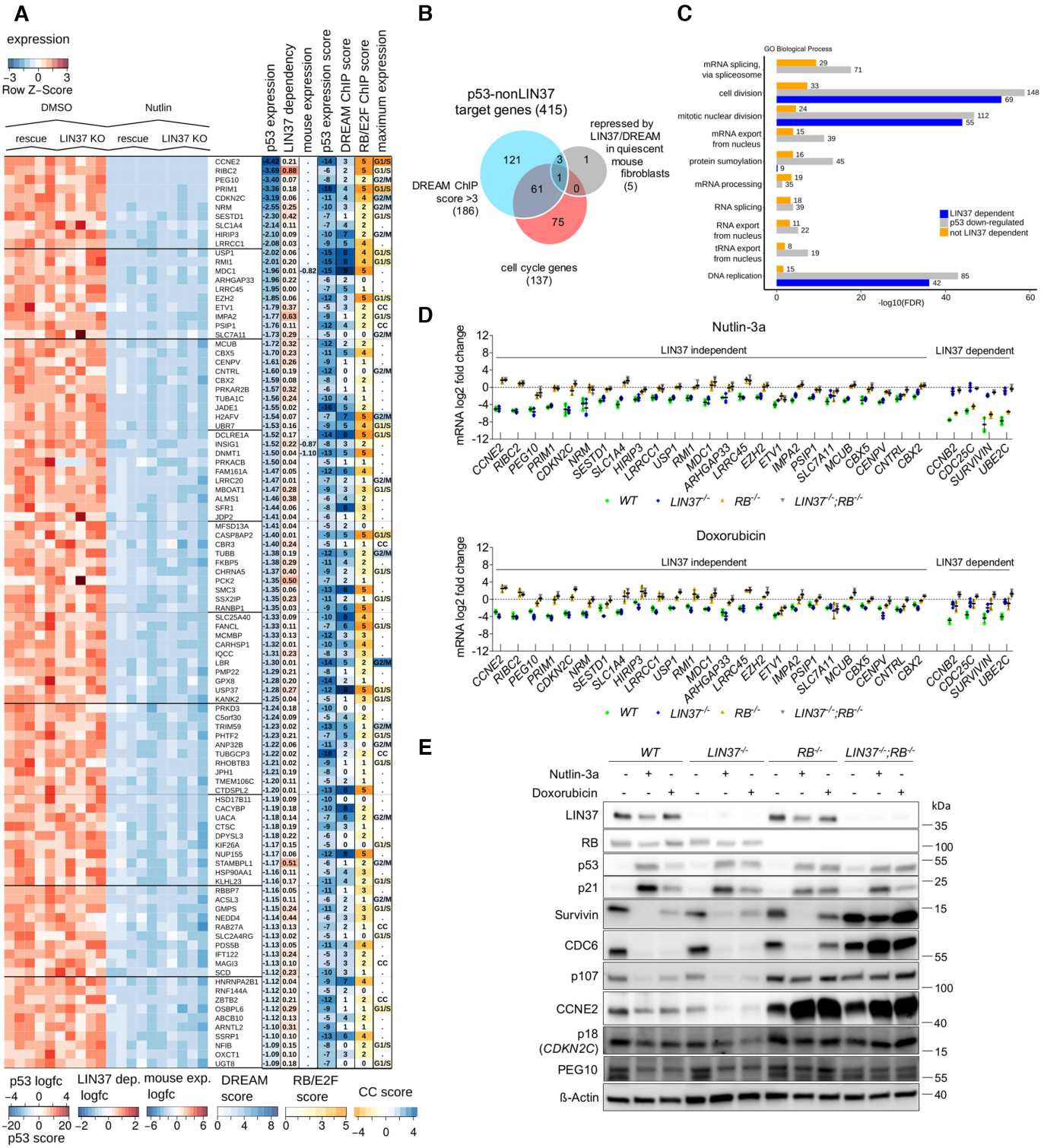

Figure 5. Identification of genes repressed by p53 independent of LIN37/DREAM. (**A**) Heat map of genes downregulated upon Nutlin-3a treatment independently of LIN37. Color code and arrangement of columns as described in Figure 3. (**B**) Venn diagram of genes downregulated upon Nutlin-3a treatment in a LIN37-independent manner. The overlap of genes with DREAM ChIP score >3, genes repressed by LIN37 in mouse fibroblasts and known cell-cycle genes is shown. (**C**) False discovery rate (FDR) of top 10 GO term (Gene Ontology Biological Process) enrichment of genes downregulated upon Nutlin-3a treatment (grey), by Nutlin-3a in a LIN37-dependent (blue), and independent (orange) manner. The number of respective genes is written to the right of the bars. (**D**) HCT116 wild-type (WT) and knockout (*LIN37*$^{-/-}$, *RB*$^{-/-}$, *LIN37*$^{-/-}$;*RB*$^{-/-}$) cells were treated with Nutlin-3a or doxorubicin for 48 h. Untreated or DMSO-treated cells served as controls. Expression of the top 25 LIN37 independent genes shown in (A) and of G_2/M genes (LIN37 dependent) was analyzed by RT-qPCR. The log2 fold changes of mRNA expression of treated vs. control cells (two biological and two technical replicates) is given. Mean values are illustrated by black bars. (**E**) HCT116 wild-type (WT) and knockout cells were treated with DMSO, Nutlin-3a, or doxorubicin for 48 h. Protein levels were analyzed by western blot and β-Actin levels served as loading control.

pressed more than 4-fold, while all top 100 genes downregulated by p53 in a LIN37-dependent manner were repressed more than 6-fold (Figure 3E). The smaller repression was also reflected by higher p53 expression scores, and except for three, these genes were also not downregulated in a Lin37-dependent manner in quiescent NIH3T3 mouse fibroblasts. Furthermore, we found generally lower DREAM ChIP binding scores as well as a smaller number of cell-cycle genes enriched in the fraction of genes repressed independent of LIN37 (Figures 3E and 5A). These observations do not only account for the top 100 genes repressed by p53 independent of LIN37, but for the whole set of 415 high probability genes (Figure 5B). GO enrichment analyses for these genes revealed that 10 biological processes were overrepresented. Several RNA-related processes were enriched (e.g. RNA splicing, RNA export from the nucleus, mRNA processing), which was a specific feature of genes downregulated independent of LIN37 (Figure 5C, Supplementary Table S3). Two cell cycle-related processes (cell division, mitotic nuclear division) were also identified, but with lower *P*-value significance compared to the set of genes downregulated in a LIN37-dependent manner.

Next, we tested the top 25 genes downregulated by p53 in a LIN37-independent manner for their expression individually by RT-qPCR in wild-type, *LIN37*$^{-/-}$, *RB*$^{-/-}$, and *LIN37*$^{-/-}$;*RB*$^{-/-}$ cells upon Nutlin-3a or doxorubicin treatment. Consistent with the RNA-seq results, these genes were similarly repressed in wild-type and *LIN37*$^{-/-}$ cells. In contrast, *RB*$^{-/-}$ cells lost the potential to downregulate these genes except for *ETV1*, *SLC7A11* and *CNTRL*. Some genes such as *CCNE2*, *RIBC2* and *SLC1A4* were even slightly activated which is in accordance with the RNA-seq data. Additional loss of LIN37 in *LIN37*$^{-/-}$;*RB*$^{-/-}$ cells led to a slight further deregulation of some genes (Figure 5D). We also analyzed protein expression of some of the identified p53-RB target genes: *CCNE2*, *CDKN2C/p18* and *PEG10* (Figure 5E). While CCNE2 protein levels were reduced in Nutlin- and doxorubicin-treated wild-type and *LIN37*$^{-/-}$ cells, they increased in *RB*$^{-/-}$ as well as in *LIN37*$^{-/-}$;*RB*$^{-/-}$ cells. Also, p18 and PEG10 repression was much more pronounced in wild-type and *LIN37*$^{-/-}$ cells than in *RB*$^{-/-}$ or *LIN37*$^{-/-}$;*RB*$^{-/-}$ cells. Furthermore, we analyzed expression of RBL1/p107 because we noticed that loss of LIN37 influenced p53-mediated mRNA expression only to a small extend while loss of RB led to an almost complete deregulation (Figure 4A). Consistent with the mRNA data, p107 protein is also expressed upon p53 activation in *RB*$^{-/-}$ or *LIN37*$^{-/-}$;*RB*$^{-/-}$ cells (Figure 5E).

Thus, these results suggest that a considerable number of genes repressed by p53 independent of LIN37/DREAM require RB for their downregulation. Moreover, there is a small set of genes that is weakly repressed by p53 independently of both DREAM and RB-E2F complexes.

Loss of gene repression in *LIN37*$^{-/-}$;*RB*$^{-/-}$ cells is phenocopied by p53 or p21 knockout

To substantiate that the observed effects were dependent on p53 and p21, we treated *p53*$^{-/-}$ or *p21*$^{-/-}$ HCT116 cells with Nutlin-3a or doxorubicin for 48 h. mRNA expression of several genes with maximal expression in G_2/M or G_1/S and genes repressed by p53 independent of LIN37 was measured by qPCR. As in *LIN37*$^{-/}$;*RB*$^{-/-}$ cells, repression of all analyzed genes was completely abrogated in *p53*$^{-/-}$ as well as in *p21*$^{-/-}$ cells (Figure 6A). The loss of mRNA downregulation also translated into a decrease in protein levels (Figure 6B). Treatment of *p53*$^{-/-}$ and *p21*$^{-/-}$ cells with Nutlin-3a did not lead to cell-cycle arrest as 2n, S phase and 4n cell populations were essentially unchanged in comparison to DMSO control treated cells (Figure 6C and D). This observation differs from the results generated with Nutlin-treated *LIN37*$^{-/-}$;*RB*$^{-/-}$ cells which show an impaired G_1 arrest, but still accumulate in G_2. In contrast, treatment with doxorubicin resulted in a loss of G_1 arrest and strong accumulation in G_2 in *p53*$^{-/-}$, *p21*$^{-/-}$ and *LIN37*$^{-/-}$;*RB*$^{-/-}$ cells (Figures 4E, F and 6C, D).

DISCUSSION

The DREAM repressor complex is a central transcriptional regulator (24,25), and its formation can be induced by p53 (7). A question of great importance is which genes are controlled by the p53-DREAM pathway and how this regulation controls cell-cycle arrest. Another main aspect of this control system is whether the p53-dependent function of the RB retinoblastoma tumor suppressor competes, overlaps, or synergizes with the p53-DREAM pathway.

In this study, we apply a knockout strategy with two arms to elucidate the impact of the p53-DREAM pathway. One arm employs LIN37 knockouts to remove DREAM repressor function (32). The second arm uses deletion of RB. Individual and double knockouts of LIN37 and RB can distinguish the specific functions of DREAM and RB in the p53 pathway.

For the first time, we provide a global analysis of genes regulated through the p53-DREAM pathway in human cells. Furthermore, we identify genes that are downregulated by p53 independently of DREAM and provide evidence that repression of many of these genes depends on RB. We show that both DREAM and RB are essential in these cells to mediate cell-cycle gene repression and cell-cycle arrest in response to p53 activation.

LIN37 deletion allows defining DREAM targets downregulated upon p53 activation

It has been shown that binding of DREAM components to target promoters coincides with p53 activation and downregulation of these genes (2,6,49). However, it remained unclear which genes are truly controlled by DREAM upon p53 activation.

Here, we identify a set of 268 high probability p53-DREAM target genes in human HCT116 cells (Figure 3, Table 1). Given that we only included genes that were identified as p53-regulated genes in various cell types following different treatments (2), this most likely reflects a general regulatory pathway. Essentially all of these gene promoters are bound by DREAM but not p53 (Figure 3). These results support the notion that transcriptional repression by p53 is indirect (2,6,8).

Generally, we find the most substantial loss of p53-dependent repression by LIN37 knockout in genes with

Table 2. 415 genes repressed by p53 independent of LIN37/DREAM

AARS	*CBFB*	*CSPP1*	*ETS2*	*H2AFV*	*JADE1*	*MBNL1*	*NUP155*	*PPP3R1*	*RPS6KA3*	*SMC3*	*TCF7L1*	*UACA*
ABCB10	*CBR3*	*CTCF*	*ETV1*	*HACD2*	*JDP2*	*MBOAT1*	*NUP188*	*PRELID1*	*S100PBP*	*SMC5*	*TCHP*	*UBR7*
ABHD2	*CBX2*	*CTDSP1*	*EXOC6*	*HAUS2*	*JPH1*	*MCMBP*	*NUP54*	*PRIM1*	*SCD*	*SMCHD1*	*TEAD4*	*UGT8*
ACSL3	*CBX3*	*CTDSPL2*	*EXOSC2*	*HDAC1*	*KANK2*	*MCUB*	*NUP58*	*PRKACB*	*SCMH1*	*SMPD4*	*TFDP1*	*USP1*
ACTL6A	*CBX5*	*CTSC*	*EXPH5*	*HDGF*	*KAT7*	*MDC1*	*NUP62*	*PRKAR2B*	*SEC22C*	*SMS*	*THNSL1*	*USP37*
ADIPOR2	*CCNE2*	*CUL3*	*EZH2*	*HIRIP3*	*KATNAL1*	*MDM1*	*NUP88*	*PRKD3*	*SENP1*	*SNRNP40*	*THOC1*	*USP39*
ADNP	*CCT5*	*CWC27*	*FABP5*	*HLTF*	*KCTD3*	*MFSD13A*	*OSBPL6*	*PRKDC*	*SEPHS1*	*SNRPB*	*THRAP3*	*UTP20*
ALMS1	*CD320*	*CYP51A1*	*FAF1*	*HMGCS1*	*KDM1A*	*MGST1*	*OXCT1*	*PSIP1*	*SESTD1*	*SNRPD1*	*TIFA*	*WDYHV1*
ANAPC1	*CDC27*	*DARS2*	*FAM161A*	*HNRNPA1*	*KHDRBS1*	*MKS1*	*PAFAH1B3*	*PSMG1*	*SET*	*SPATA33*	*TIPIN*	*XPO7*
ANKRD28	*CDK4*	*DCAF1*	*FAM20B*	*HNRNPA2B1*	*KHSRP*	*MLKL*	*PAICS*	*PTBP1*	*SF1*	*SRRM1*	*TLK1*	*XPOT*
ANO6	*CDKAL1*	*DCLRE1A*	*FAM20C*	*HNRNPA3*	*KIF26A*	*MPP6*	*PARP1*	*PTGES3*	*SF3B3*	*SRSF1*	*TMCO3*	*XYLB*
ANP32B	*CDKN2C*	*DCPS*	*FAM57A*	*HNRNPAB*	*KIF2A*	*MRPS18B*	*PATZ1*	*QSER1*	*SFPQ*	*SRSF10*	*TMEM106C*	*YARS*
ARHGAP33	*CEBPG*	*DCTPP1*	*FANCL*	*HNRNPD*	*KLHL23*	*MRPS34*	*PAXIP1*	*R3HDM1*	*SFR1*	*SRSF2*	*TMEM109*	*YWHAH*
ARNTL2	*CEBPZ*	*DGCR8*	*FARSB*	*HNRNPF*	*KPNB1*	*MTERF3*	*PAXX*	*RAB27A*	*SFXN1*	*SRSF3*	*TMEM18*	*ZBTB14*
ASRGL1	*CENPV*	*DHCR7*	*FBXO17*	*HNRNPH1*	*LANCL1*	*MTMR2*	*PCK2*	*RAB8A*	*SH3PXD2B*	*SRSF7*	*TMEM38B*	*ZBTB2*
ATF4	*CENPX*	*DHX15*	*FERMT2*	*HNRNPH3*	*LBR*	*MYH10*	*PDS5A*	*RAI14*	*SHMT2*	*SSBP3*	*TNPO3*	*ZNF148*
ATP11C	*CEP170*	*DIAPH1*	*FKBP4*	*HNRNPM*	*LIMS1*	*NAA15*	*PDS5B*	*RALGPS2*	*SIN3A*	*SSRP1*	*TOP3A*	*ZNF184*
ATP2B1	*CEP70*	*DIS3L*	*FKBP5*	*HNRNPR*	*LIN52*	*NBN*	*PEG10*	*RAN*	*SKIV2L2*	*SSX2IP*	*TRA2B*	*ZNF395*
AZIN1	*CHD1*	*DLAT*	*FKBPL*	*HNRNPU*	*LONP1*	*NCOA5*	*PHF13*	*RANBP1*	*SLBP*	*STAG1*	*TRAF2*	*ZNF639*
BAG2	*CHD4*	*DLG3*	*FUS*	*HP1BP3*	*LRP8*	*NEDD4*	*PHLPP1*	*RAP1GDS1*	*SLC1A4*	*STAG2*	*TRIB3*	
BAZ1B	*CHRAC1*	*DNAJC1*	*FZD7*	*HPRT1*	*LRRC20*	*NEK1*	*PHLPP2*	*RAPH1*	*SLC1A5*	*STAMBPL1*	*TRIM59*	
BCLAF1	*CHRNA5*	*DNAJC15*	*GALNT14*	*HS2ST1*	*LRRC45*	*NEK3*	*PHTF2*	*RBBP4*	*SLC20A1*	*STIP1*	*TSEN15*	
BDH1	*CKAP5*	*DNMT1*	*GARS*	*HSD17B11*	*LRRC58*	*NFIB*	*PIGU*	*RBBP7*	*SLC25A40*	*STRBP*	*TTC26*	
BEND3	*CLIC4*	*DPYSL3*	*GJC1*	*HSP90AA1*	*LRRC8C*	*NIN*	*PLEK2*	*RDX*	*SLC2A4RG*	*STX2*	*TTLL4*	
BNIP1	*CLN6*	*DTD1*	*GMPS*	*HSPD1*	*LRRCC1*	*NONO*	*PLP2*	*RFC1*	*SLC38A1*	*SUPT16H*	*TUBA1C*	
BRI3BP	*CNOT9*	*DYRK1A*	*GNB1*	*HSPE1*	*MAD2L2*	*NOP58*	*PLPP2*	*RHEB*	*SLC3A2*	*SYNCRIP*	*TUBB*	
BUB3	*CNTRL*	*EBAG9*	*GPR180*	*ICMT*	*MAGI3*	*NPAT*	*PMF1*	*RHOBTB3*	*SLC43A1*	*TAF5L*	*TUBB2B*	
C12orf65	*CNTROB*	*EHMT2*	*GPRC5B*	*IFT122*	*MAGOHB*	*NRF1*	*PMP22*	*RIBC2*	*SLC44A1*	*TBL1X*	*TUBG1*	
C5orf30	*COLGALT1*	*EIF4EBP1*	*GPT2*	*IMPA2*	*MANEA*	*NRM*	*POGZ*	*RIF1*	*SLC4A7*	*TBL1XR1*	*TUBGCP3*	
CACYBP	*COMMD10*	*EML4*	*GPX8*	*INSIG1*	*MANEAL*	*NSD3*	*POLD2*	*RMI1*	*SLC7A1*	*TCAF1*	*TUBGCP4*	
CAND1	*COQ7*	*ENAH*	*GRK6*	*INTS7*	*MAP3K4*	*NUCKS1*	*POT1*	*RNF138*	*SLC7A11*	*TCEA1*	*TWISTNB*	
CARHSP1	*CPSF6*	*ENOSF1*	*GULP1*	*IPO9*	*MARS*	*NUDC*	*POU2F1*	*RNF144A*	*SLF2*	*TCF12*	*TXLNG*	
CASP8AP2	*CS*	*ERLIN1*	*H1FX*	*IQCC*	*MAZ*	*NUDT21*	*PPIF*	*ROCK2*	*SMARCA5*	*TCF3*	*TYRO3*	

Genes were selected by the following criteria: (I) significantly repressed by p53 ($P_{adj} < 0.001$), (II) no decreased repression in *LIN37*$^{-/-}$ cells ($\Delta\log_2$FC > 0), and (III) p53 expression score ≤ -5.

maximum expression in G_2/M (Figure 3, Supplementary Table S2). p53-dependent repression of G_2/M genes is regulated through CHR promoter elements that can only bind DREAM, while G_1/S genes bind DREAM as well as RB-E2F complexes through E2F sites (26). Thus, binding of RB-E2F complexes to G_1/S gene promoters may at least partially compensate for loss of DREAM function (Figures 4 and 5).

Interestingly, we find a vast overlap between the set of p53-LIN37/DREAM target genes and genes repressed by Lin37/DREAM in quiescent mouse fibroblasts (Figure 3, Supplementary Table S2). This observation indicates the conservation of the DREAM-dependent pathway leading to transcriptional repression in response to multiple growth limiting signals. This notion is further supported by a remarkable phylogenetic conservation of CHR and E2F promoter elements in mammalian cell-cycle gene promoters (28).

Many genes downregulated by p53 independent of LIN37 require RB

In the transcriptome analysis, we identify 1698 genes that were significantly repressed upon activation of p53 with Nutlin-3a. In 708 of these genes, repression is weaker in *LIN37*$^{-/-}$ cells (Δlog2FC<0) than in wild-type cells, while 990 genes are still significantly downregulated in *LIN37*$^{-/-}$ cells (Δlog2FC>0) (Figure 3, Supplementary Table S2). Thus, more than half of the genes repressed by p53 were downregulated in a LIN37/DREAM-independent manner (Figure 3). In the high-probability subset (Table 2), we find that cell cycle-related genes are still enriched, but much less than in the sets of p53- or LIN37-p53-target genes (compare Figures 3H and 5C). By analyzing the regulation of the top 25 genes most substantially repressed by p53 independently of LIN37, we found that repression of most of these genes relies on RB (Figs 5D and 5E). One of the most prominent examples of these cell-cycle genes is *CCNE2*. This gene was substantially repressed by p53 in LIN37-expressing cells (log2FC = -4.4), but also in *LIN37*$^{-/-}$ cells (log2FC = -4.6). These results are consistent with earlier reports that found *Cyclin E* expression to be considerably upregulated in *RB*$^{-/-}$ cells (33,53–55), but not in *p107*$^{-/-}$*;p130*$^{-/-}$ MEFs (33). Interestingly, the deregulation of *CCNE2* expression in *RB*$^{-/-}$ cells upon p53 activation did not lead to increased proliferation and DNA replication as shown for *CCNE* overexpression in senescent IMR90 cells with reduced RB expression (55).

In a recently published report that investigated serum-starved fibroblasts, no evidence was found for cell-cycle genes that are exclusively regulated by RB (56). In contrast, our data reveal that a substantial set of genes is solely repressed by RB and not by DREAM after p53 activation (Figure 5). In addition to different cell types and treatments that have been employed, the different findings may also stem from remaining p130 and p107 in the experimental setup of Schade and colleagues. In general, a more detailed analysis of genes repressed by RB and not by DREAM may help to explain differences in tumor suppressor potency between RB and p107/p130.

Both RB and DREAM are necessary for the repression of G_1/S and G_2/M cell-cycle genes

We have shown that DREAM binds to CHR elements of G_2/M genes as well as to E2F sites of G_1/S genes (26).

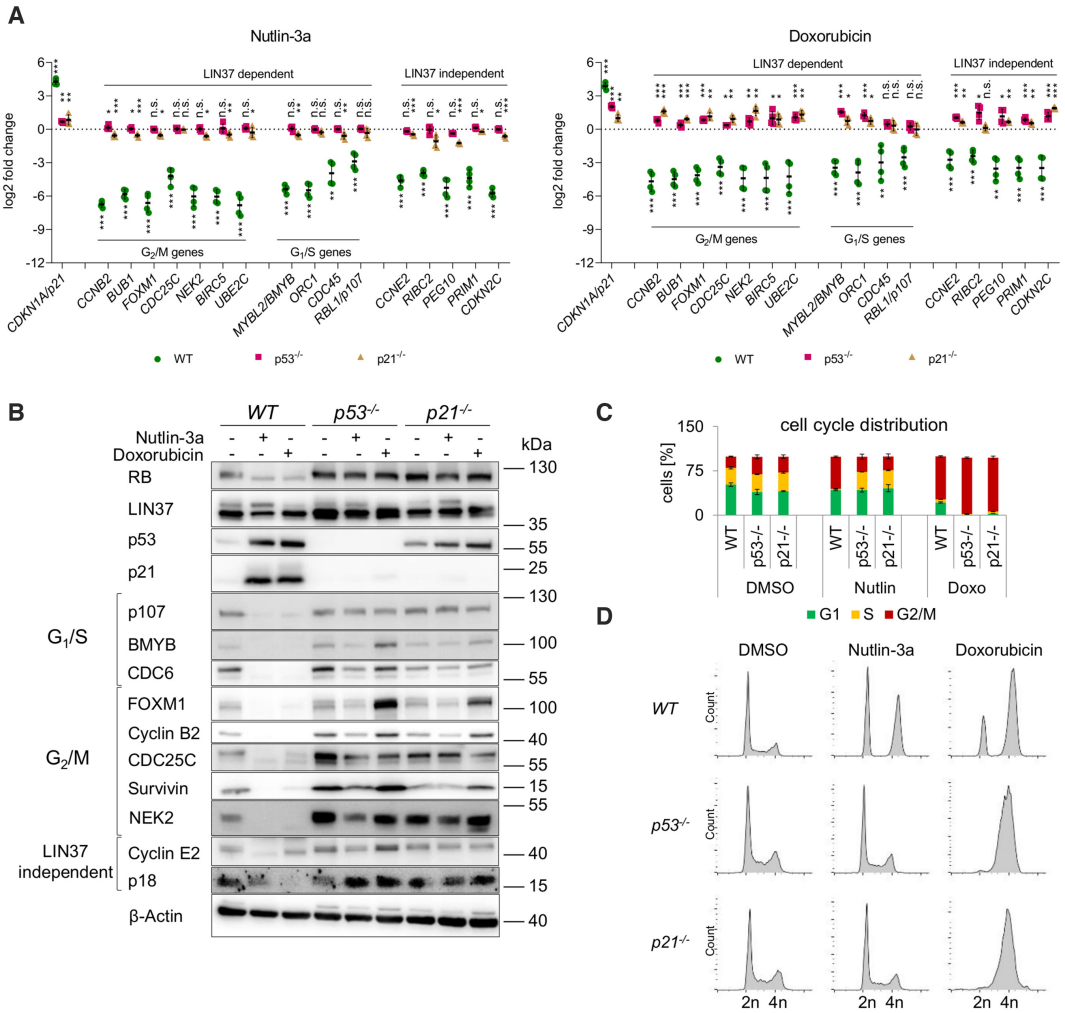

Figure 6. *p53*$^{-/-}$ and *p21*$^{-/-}$ HCT116 cells cannot downregulate cell-cycle gene expression on mRNA and protein levels in response to treatment with Nutlin-3a or doxorubicin. (**A**) HCT116 wild-type, *p53*$^{-/-}$, and *p21*$^{-/-}$ cells were treated with DMSO, Nutlin-3a or doxorubicin for 48 h. mRNA expression of *CDKN1A/p21*, G_2/M- and G_1/S-specific genes as well as LIN37-independently regulated genes were measured by RT-qPCR. The log2 fold changes of mRNA expression of treated vs. control cells are given. Mean values of two biological and two technical replicates are indicated by black bars. Significances were calculated with the Student's T-Test (n.s. – not significant, $^{*}P \leq .05$, $^{**}P \leq .01$, $^{***}P \leq .001$). (**B**) Protein expression in response to 48 h of Nutlin-3a or doxorubicin treatment in HCT116 wild-type (WT), *p53*$^{-/-}$, and *p21*$^{-/-}$ HCT116 cells were analyzed by western blot. β-Actin served as a loading control. (**C**) Cell-cycle distribution of cell lines analyzed in (A) was measured by flow cytometry after propidium iodide staining. Mean values ±SD of two biological replicates are given. (**D**) Histograms of one representative experiment shown in (C) are given.

In contrast, RB-E2F complexes can only interact with E2F sites because they lack the CHR-binding component LIN54 to bind CHR sites (2,26,28,57). Our results support a model in which loss of DREAM function leads to derepression of both G_1/S and G_2/M genes. Deregulation is more pronounced for G_2/M genes because DREAM-dependent loss of G_1/S gene repression may be compensated in part by RB-E2F control. One could also hypothesize that loss of RB may only influence repression of G_1/S genes because of its inability to regulate G_2/M genes through CHR elements. However, our data show that loss of RB also leads to a reduced repression of G_2/M genes (Figure 4). These findings are in agreement with our earlier results that showed derepression of G_2/M genes in serum-starved *RB*$^{-/-}$ NIH3T3 cells (32). Thus, RB is required for full repression of these genes, even though RB binding is not detected at promoters of the vast majority of G_2/M genes (2,28), which suggests an indirect mechanism. This is especially interesting since we (Figures 4 and 5) and others (52,58–61) find RB protein expression considerably reduced upon treatment with Nutlin-3a or doxorubicin.

One report suggested that functional RB is not required for p21-dependent repression of p53 target genes (49). This statement was made based on work from Saos-2 cells, which carry non-functional RB and still show repression of G_2/M genes with ~2-fold repression of *BIRC5/Survivin* and *CDC25C*. However, it remains unclear whether re-expression of RB in Saos-2 cells would reinforce this weak repression which then would be in agreement with our data. Given that overexpression of B-MYB was shown to disrupt the DREAM complex leading to activation of gene expression dependent on CHR elements (31), the lack of G_2/M gene repression in RB-negative cells upon doxorubicin treatment may be caused by an increased B-MYB pro-

tein expression (Figure 4C). Interestingly, it was also shown that cells expressing high levels of ectopically expressed B-MYB can enter S phase, even when the p53-p21 pathway is activated (62). As B-MYB overexpression antagonizes DREAM, these observations are in line with our results showing that *LIN37*$^{-/-}$ cells lacking DREAM function do not properly arrest in G_1 following induction of p53 (Figure 4). Furthermore, the persisting expression of B-MYB in Nutlin-3a- or doxorubicin-treated *LIN37*$^{-/-}$;*RB*$^{-/-}$ cells may be central for attenuating the G_1/S checkpoint.

Generally, we find that p53-dependent mRNA downregulation of many cell-cycle genes is compromised in *LIN37*$^{-/-}$ or *RB*$^{-/-}$ cells which results in similar expression with or without activation of p53. However, often protein levels do not follow this deregulation and they are still decreased after p53 activation (Figure 4). Interestingly, combined knockout of *LIN37* and *RB* only leads to a minor additional increase of mRNA abundance in comparison to single knockout cells, but protein expression of all analyzed genes is not reduced upon p53 activation (e.g. CCNB2, Figure 4). The observation that only a combined loss of DREAM and RB function leads to a complete deregulation of p53-dependent cell-cycle gene expression, as observed in *p53*$^{-/-}$ and *p21*$^{-/-}$ cells (Figure 6) indicates that both complexes can at least partially substitute for each other. However, it remains elusive whether only in the double knockout cells a certain mRNA threshold is exceeded which then leads to robust protein expression, or whether other non-transcriptional mechanisms like the regulation of protein stability are involved. Together, our data provide evidence that both DREAM and RB are essential for the repression of many G_1/S and G_2/M cell-cycle genes by direct as well as indirect mechanisms.

DREAM and RB cooperate in p53-mediated cell-cycle arrest

In all wild-type and knockout HCT116 cell lines analyzed, we find a more pronounced G_2 arrest after doxorubicin treatment compared to Nutlin-3a (Figures 4 and 6). Nutlin-3a treatment leads to increased p53 levels by binding the E3 ubiquitin-protein ligase MDM2 in the p53-binding pocket, which results in reduced p53 degradation and thus activation of the p53 pathway (63). In contrast to this rather specific mechanism, doxorubicin intercalates into DNA and inhibits the progression of topoisomerase II, which induces DNA damage especially in S phase when cells have already passed the G_1 checkpoint (64). Furthermore, DNA damage activates multiple pathways that trigger G_2 arrest in a p53-dependent, but also independent manner. For example, cells can arrest in G_2 independent of p53 through activating the ATM/CHK2/Cdc25 or ATR/CHK1/Cdc25 pathways (65). Thus, doxurubicin-induced DNA damage activates the G_2 checkpoint more robustly than p53 induction by Nutlin-3a.

Loss of LIN37 led to a reduction of the G_1 population in both HCT116 and C2C12 cells and an increase of the G_2 fraction upon p53 activation (Figures 1, 2, 4) indicating a compromised regulation of the G_1 checkpoint. This observation was not made in *RB*$^{-/-}$ HCT116 cells (Figure 4). However, additional loss of RB in *LIN37*$^{-/-}$ cells led to a further decrease of G_1 and increase of G_2 cell populations. Most strikingly, only combined loss of LIN37 and RB resulted in the occurance of EdU-positive S phase cells upon treatment with Nutlin-3a or doxorubicin (Figure 4F), indicating that single knockout HCT116 cells can still efficiently arrest in G_2 in contrast to the double knockouts. These findings are in agreement with earlier reports. For example, *p130*$^{-/-}$;*p107*$^{-/-}$ MEFs treated with doxorubicin for 24 h arrested in G_1 and G_2 like wild-type cells, while pocket protein triple knockouts lost this ability (29). Interestingly, *RB*$^{-/-}$ MEFs were defective in cell-cycle arrest after gamma-irradiation or treatment with several DNA-damaging agents, while *p130*$^{-/-}$;*p107*$^{-/-}$ MEFs did not show such defects (66). In contrast, shRNA-mediated reduction of p130 levels led to a defective doxorubicin-induced G_1 arrest in a human glioblastoma cell line and in human fibroblasts (52). In our experimental setting, only a combined abrogation of DREAM and RB function led to a loss of cell-cycle arrest and the occurrence of DNA replicating cells (Figure 4). However, in comparison to *p53*$^{-/-}$ and *p21*$^{-/-}$ cells that completely lost their ability to halt the cell cycle upon Nutlin-3a treatment (Figure 6), a clear decrease of S phase cells and an accumulation of G_2 cells was still observed in *LIN37*$^{-/-}$;*RB*$^{-/-}$ cells (Figure 4). It remains to be shown to which extent transcription-dependent or -independent functions of DREAM and RB are central for p53-mediated cell-cycle arrest. For example, RB is also involved in the regulation of protein stability, e.g. by stabilizing the CDK inhibitor p27 through the inactivation of Skp2 (67,68) and chromatin remodeling (69). Furthermore, p107/p130 may at least partially compensate for RB functions in *RB*$^{-/-}$ and *LIN37*$^{-/-}$;*RB*$^{-/-}$ cells. Given that both p53 and p21 are required for sustained G_2 arrest (37), p21-mediated inhibition of CDK activity may be sufficient to arrest the cell cycle at the G_2/M checkpoint even when DREAM and RB are not available. However, failure to downregulate CDK1 expression (Table 1) likely requires continuously high p21 levels, which are known to vary in the p53 response (70) potentially leading to cells slipping the arrest when p21 levels are low.

Taken together, we show that DREAM and RB are key factors in the p53 signaling pathway to downregulate a large number of cell-cycle genes and to arrest the cell cycle at the G_1/S transition.

DATA AVAILABILITY

RNA-Seq data generated for this publication was deposited at the European Nucleotide Archive as study PRJEB31044.

SUPPLEMENTARY DATA

Supplementary Data are available at NAR Online.

ACKNOWLEDGEMENTS

The authors thank Carola Koschke and Victoria Menger for technical assistance. Andreas Lösche and Kathrin Jäger performed flow cytometry analyses at the IZKF Leipzig Fluorescence Technologies Core Unit. Knut Krohn and Birgit Oelzner performed Sanger Sequencing at the IZKF Leipzig DNA Technologies Core Unit. The assistance of

Ivonne Goerlich in next-generation sequencing at the FLI DNA Sequencing Core Facility is gratefully acknowledged. We thank Seth Rubin for comments that greatly improved the manuscript. GAM thanks Sunna Hauschildt for enlightening discussions and Bahriye Aktas for supporting his research.

Authors contributions: G.A.M. conceived and supervised the study. S.H.B. performed the computational analyses. M.F. and S.H. supervised the RNA-seq analyses. S.U., G.A.M., C.F.S.M. and R.K. performed all other experiments. G.A.M. with the help of S.H.B., K.E., M.F., S.U. and P.F.S. wrote the manuscript. All authors read and approved the final manuscript.

FUNDING

German Research Foundation (DFG) [MU 3798/1-1 to G.A.M.]; MF [FI 1993/2-1]; German BMBF (ICGC-Data Mining) [01KU1505-C to S.H.B. and S.H.]; Medical School, University of Leipzig (to K.E.); German Academic Scholarship Foundation (Studienstiftung des deutschen Volkes to S.U.); Christiane Nüsslein-Volhard Foundation (to S.U.). Funding for open access charge: German Research Foundation (DFG) and Universität Leipzig within the program of Open Access Publishing.

Conflict of interest statement. None declared.

REFERENCES

1. Kastenhuber,E.R. and Lowe,S.W. (2017) Putting p53 in Context. *Cell*, **170**, 1062–1078.
2. Fischer,M., Grossmann,P., Padi,M. and DeCaprio,J.A. (2016) Integration of TP53, DREAM, MMB-FOXM1 and RB-E2F target gene analyses identifies cell cycle gene regulatory networks. *Nucleic Acids Res.*, **44**, 6070–6086.
3. Fischer,M. (2017) Census and evaluation of p53 target genes. *Oncogene*, **36**, 3943–3956.
4. Engeland,K. (2018) Cell cycle arrest through indirect transcriptional repression by p53: I have a DREAM. *Cell Death Differ.*, **25**, 114–132.
5. Nguyen,T.T., Grimm,S.A., Bushel,P.R., Li,J., Li,Y., Bennett,B.D., Lavender,C.A., Ward,J.M., Fargo,D.C., Anderson,C.W. *et al.* (2018) Revealing a human p53 universe. *Nucleic Acids Res.*, **46**, 8153–8167.
6. Fischer,M., Steiner,L. and Engeland,K. (2014) The transcription factor p53: not a repressor, solely an activator. *Cell Cycle*, **13**, 3037–3058.
7. Mannefeld,M., Klassen,E. and Gaubatz,S. (2009) B-MYB is required for recovery from the DNA damage-induced G2 checkpoint in p53 mutant cells. *Cancer Res.*, **69**, 4073–4080.
8. Quaas,M., Müller,G.A. and Engeland,K. (2012) p53 can repress transcription of cell cycle genes through a p21(WAF1/CIP1)-dependent switch from MMB to DREAM protein complex binding at CHR promoter elements. *Cell Cycle*, **11**, 4661–4672.
9. Dulic,V., Kaufmann,W.K., Wilson,S.J., Tlsty,T.D., Lees,E., Harper,J.W., Elledge,S.J. and Reed,S.I. (1994) p53-dependent inhibition of cyclin-dependent kinase activities in human fibroblasts during radiation-induced G1 arrest. *Cell*, **76**, 1013–1023.
10. Harper,J.W., Adami,G.R., Wei,N., Keyomarsi,K. and Elledge,S.J. (1993) The p21 Cdk-interacting protein Cip1 is a potent inhibitor of G1 cyclin-dependent kinases. *Cell*, **75**, 805–816.
11. Harper,J.W., Elledge,S.J., Keyomarsi,K., Dynlacht,B., Tsai,L.H., Zhang,P., Dobrowolski,S., Bai,C., Connell-Crowley,L., Swindell,E. *et al.* (1995) Inhibition of cyclin-dependent kinases by p21. *Mol. Biol. Cell*, **6**, 387–400.
12. O'Leary,B., Finn,R.S. and Turner,N.C. (2016) Treating cancer with selective CDK4/6 inhibitors. *Nat. Rev. Clin. Oncol.*, **13**, 417–430.
13. Sherr,C.J. and Roberts,J.M. (1995) Inhibitors of mammalian G1 cyclin-dependent kinases. *Genes Dev.*, **9**, 1149–1163.
14. Beijersbergen,R.L., Carlee,L., Kerkhoven,R.M. and Bernards,R. (1995) Regulation of the retinoblastoma protein-related p107 by G1 cyclin complexes. *Genes Dev.*, **9**, 1340–1353.
15. Bruce,J.L., Hurford,R.K. Jr, Classon,M., Koh,J. and Dyson,N. (2000) Requirements for cell cycle arrest by p16INK4a. *Mol. Cell*, **6**, 737–742.
16. Helin,K., Lees,J.A., Vidal,M., Dyson,N., Harlow,E. and Fattaey,A. (1992) A cDNA encoding a pRB-binding protein with properties of the transcription factor E2F. *Cell*, **70**, 337–350.
17. Lees,J.A., Saito,M., Vidal,M., Valentine,M., Look,T., Harlow,E., Dyson,N. and Helin,K. (1993) The retinoblastoma protein binds to a family of E2F transcription factors. *Mol. Cell Biol.*, **13**, 7813–7825.
18. Liban,T.J., Medina,E.M., Tripathi,S., Sengupta,S., Henry,R.W., Buchler,N.E. and Rubin,S.M. (2017) Conservation and divergence of C-terminal domain structure in the retinoblastoma protein family. *Proc. Natl. Acad. Sci. U.S.A.*, **114**, 4942–4947.
19. Liban,T.J., Thwaites,M.J., Dick,F.A. and Rubin,S.M. (2016) Structural conservation and E2F binding specificity within the retinoblastoma pocket protein family. *J. Mol. Biol.*, **428**, 3960–3971.
20. Litovchick,L., Sadasivam,S., Florens,L., Zhu,X., Swanson,S.K., Velmurugan,S., Chen,R., Washburn,M.P., Liu,X.S. and DeCaprio,J.A. (2007) Evolutionarily conserved multisubunit RBL2/p130 and E2F4 protein complex represses human cell cycle-dependent genes in quiescence. *Mol. Cell*, **26**, 539–551.
21. Pilkinton,M., Sandoval,R. and Colamonici,O.R. (2007) Mammalian Mip/LIN-9 interacts with either the p107, p130/E2F4 repressor complex or B-Myb in a cell cycle-phase-dependent context distinct from the Drosophila dREAM complex. *Oncogene*, **26**, 7535–7543.
22. Schmit,F., Korenjak,M., Mannefeld,M., Schmitt,K., Franke,C., von,E.B., Gagrica,S., Hanel,F., Brehm,A. and Gaubatz,S. (2007) LINC, a human complex that is related to pRB-containing complexes in invertebrates regulates the expression of G2/M genes. *Cell Cycle*, **6**, 1903–1913.
23. Guiley,K.Z., Liban,T.J., Felthousen,J.G., Ramanan,P., Litovchick,L. and Rubin,S.M. (2015) Structural mechanisms of DREAM complex assembly and regulation. *Genes Dev.*, **29**, 961–974.
24. Sadasivam,S. and DeCaprio,J.A. (2013) The DREAM complex: master coordinator of cell cycle-dependent gene expression. *Nat. Rev. Cancer*, **13**, 585–595.
25. Fischer,M. and Müller,G.A. (2017) Cell cycle transcription control: DREAM/MuvB and RB-E2F complexes. *Crit Rev. Biochem. Mol. Biol.*, **52**, 638–662.
26. Müller,G.A., Stangner,K., Schmitt,T., Wintsche,A. and Engeland,K. (2016) Timing of transcription during the cell cycle: Protein complexes binding to E2F, E2F/CLE, CDE/CHR, or CHR promoter elements define early and late cell cycle gene expression. *Oncotarget*, **8**, 97736–97748.
27. Müller,G.A., Quaas,M., Schumann,M., Krause,E., Padi,M., Fischer,M., Litovchick,L., DeCaprio,J.A. and Engeland,K. (2012) The CHR promoter element controls cell cycle-dependent gene transcription and binds the DREAM and MMB complexes. *Nucleic Acids Res.*, **40**, 1561–1578.
28. Müller,G.A., Wintsche,A., Stangner,K., Prohaska,S.J., Stadler,P.F. and Engeland,K. (2014) The CHR site: definition and genome-wide identification of a cell cycle transcriptional element. *Nucleic Acids Res.*, **42**, 10331–10350.
29. Jackson,M.W., Agarwal,M.K., Yang,J., Bruss,P., Uchiumi,T., Agarwal,M.L., Stark,G.R. and Taylor,W.R. (2005) p130/p107/p105Rb-dependent transcriptional repression during DNA-damage-induced cell-cycle exit at G2. *J. Cell Sci.*, **118**, 1821–1832.
30. Forristal,C., Henley,S.A., MacDonald,J.I., Bush,J.R., Ort,C., Passos,D.T., Talluri,S., Ishak,C.A., Thwaites,M.J., Norley,C.J. *et al.* (2014) Loss of the mammalian DREAM complex deregulates chondrocyte proliferation. *Mol. Cell Biol.*, **34**, 2221–2234.
31. Iness,A.N., Felthousen,J., Ananthapadmanabhan,V., Sesay,F., Saini,S., Guiley,K.Z., Rubin,S.M., Dozmorov,M. and Litovchick,L. (2018) The cell cycle regulatory DREAM complex is disrupted by high expression of oncogenic B-Myb. *Oncogene*, **38**, 1080–1092.
32. Mages,C.F., Wintsche,A., Bernhart,S.H. and Müller,G.A. (2017) The DREAM complex through its subunit Lin37 cooperates with Rb to initiate quiescence. *Elife.*, **6**, e26876.

33. Hurford,R.K., Cobrinik,D., Lee,M.H. and Dyson,N. (1997) pRB and p107/p130 are required for the regulated expression of different sets of E2F responsive genes. *Genes Dev.*, **11**, 1447–1463.
34. Sage,J., Mulligan,G.J., Attardi,L.D., Miller,A., Chen,S., Williams,B., Theodorou,E. and Jacks,T. (2000) Targeted disruption of the three Rb-related genes leads to loss of G(1) control and immortalization. *Genes Dev.*, **14**, 3037–3050.
35. Dannenberg,J.H., van,R.A., Schuijff,L. and Te,R.H. (2000) Ablation of the retinoblastoma gene family deregulates G(1) control causing immortalization and increased cell turnover under growth-restricting conditions. *Genes Dev.*, **14**, 3051–3064.
36. Classon,M., Salama,S., Gorka,C., Mulloy,R., Braun,P. and Harlow,E. (2000) Combinatorial roles for pRB, p107, and p130 in E2F-mediated cell cycle control. *Proc. Natl. Acad. Sci. U.S.A.*, **97**, 10820–10825.
37. Bunz,F., Dutriaux,A., Lengauer,C., Waldman,T., Zhou,S., Brown,J.P., Sedivy,J.M., Kinzler,K.W. and Vogelstein,B. (1998) Requirement for p53 and p21 to sustain G2 arrest after DNA damage. *Science*, **282**, 1497–1501.
38. Uphoff,C.C. and Drexler,H.G. (2002) Detection of mycoplasma in leukemia-lymphoma cell lines using polymerase chain reaction. *Leukemia*, **16**, 289–293.
39. Ran,F.A., Hsu,P.D., Lin,C.Y., Gootenberg,J.S., Konermann,S., Trevino,A.E., Scott,D.A., Inoue,A., Matoba,S., Zhang,Y. *et al.* (2013) Double nicking by RNA-guided CRISPR Cas9 for enhanced genome editing specificity. *Cell*, **154**, 1380–1389.
40. Ran,F.A., Hsu,P.D., Wright,J., Agarwala,V., Scott,D.A. and Zhang,F. (2013) Genome engineering using the CRISPR-Cas9 system. *Nat. Protoc.*, **8**, 2281–2308.
41. Kirschner,R.D., Sänger,K., Müller,G.A. and Engeland,K. (2008) Transcriptional activation of the tumor suppressor and differentiation gene S100A2 by a novel p63-binding site. *Nucleic Acids Res.*, **36**, 2969–2980.
42. Tavner,F., Frampton,J. and Watson,R.J. (2007) Targeting an E2F site in the mouse genome prevents promoter silencing in quiescent and post-mitotic cells. *Oncogene*, **26**, 2727–2735.
43. Bentley,D.R., Balasubramanian,S., Swerdlow,H.P., Smith,G.P., Milton,J., Brown,C.G., Hall,K.P., Evers,D.J., Barnes,C.L., Bignell,H.R. *et al.* (2008) Accurate whole human genome sequencing using reversible terminator chemistry. *Nature*, **456**, 53–59.
44. Martin,M. (2011) Cutadapt removes adapter sequences from high-throughput sequencing reads. *EMBnet j.*, **17**, 10.
45. Hoffmann,S., Otto,C., Doose,G., Tanzer,A., Langenberger,D., Christ,S., Kunz,M., Holdt,L.M., Teupser,D., Hackermüller,J. *et al.* (2014) A multi-split mapping algorithm for circular RNA, splicing, trans-splicing and fusion detection. *Genome Biol.*, **15**, R34.
46. Liao,Y., Smyth,G.K. and Shi,W. (2014) featureCounts: an efficient general purpose program for assigning sequence reads to genomic features. *Bioinformatics*, **30**, 923–930.
47. Love,M.I., Huber,W. and Anders,S. (2014) Moderated estimation of fold change and dispersion for RNA-seq data with DESeq2. *Genome Biol.*, **15**, 550.
48. Huang,D.W., Sherman,B.T. and Lempicki,R.A. (2009) Systematic and integrative analysis of large gene lists using DAVID bioinformatics resources. *Nat. Protoc.*, **4**, 44–57.
49. Benson,E.K., Mungamuri,S.K., Attie,O., Kracikova,M., Sachidanandam,R., Manfredi,J.J. and Aaronson,S.A. (2014) p53-dependent gene repression through p21 is mediated by recruitment of E2F4 repression complexes. *Oncogene*, **33**, 3959–3969.
50. Helin,K., Wu,C.L., Fattaey,A.R., Lees,J.A., Dynlacht,B.D., Ngwu,C. and Harlow,E. (1993) Heterodimerization of the transcription factors E2F-1 and Dp-1 leads to cooperative transactivation. *Genes & Development*, **7**, 1850–1861.
51. Flemington,E.K., Speck,S.H. and Kaelin,W. G. Jr (1993) E2F-1-mediated transactivation is inhibited by complex formation with the retinoblastoma susceptibility gene product. *Proc. Natl. Acad. Sci. U.S.A.*, **90**, 6914–6918.
52. Helmbold,H., Komm,N., Deppert,W. and Bohn,W. (2009) Rb2/p130 is the dominating pocket protein in the p53-p21 DNA damage response pathway leading to senescence. *Oncogene*, **28**, 3456–3467.
53. Herrera,R.E., Makela,T.P. and Weinberg,R.A. (1996) TGF beta-induced growth inhibition in primary fibroblasts requires the retinoblastoma protein. *Mol. Biol. Cell*, **7**, 1335–1342.
54. Herrera,R.E., Sah,V.P., Williams,B.O., Makela,T.P., Weinberg,R.A. and Jacks,T. (1996) Altered cell cycle kinetics, gene expression, and G1 restriction point regulation in Rb-deficient fibroblasts. *Mol. Cell Biol.*, **16**, 2402–2407.
55. Chicas,A., Wang,X., Zhang,C., McCurrach,M., Zhao,Z., Mert,O., Dickins,R.A., Narita,M., Zhang,M. and Lowe,S.W. (2010) Dissecting the unique role of the retinoblastoma tumor suppressor during cellular senescence. *Cancer Cell*, **17**, 376–387.
56. Schade,A.E., Oser,M.G., Nicholson,H.E. and DeCaprio,J.A. (2019) Cyclin D–CDK4 relieves cooperative repression of proliferation and cell cycle gene expression by DREAM and RB. *Oncogene*, **26**, 539.
57. Marceau,A.H., Felthousen,J.G., Goetsch,P.D., Iness,A.N., Lee,H.W., Tripathi,S.M., Strome,S., Litovchick,L. and Rubin,S.M. (2016) Structural basis for LIN54 recognition of CHR elements in cell cycle-regulated promoters. *Nat. Commun.*, **7**, 12301.
58. Du,W., Wu,J., Walsh,E.M., Zhang,Y., Chen,C.Y. and Xiao,Z.-X.J. (2009) Nutlin-3 affects expression and function of retinoblastoma protein: role of retinoblastoma protein in cellular response to nutlin-3. *J. Biol. Chem.*, **284**, 26315–26321.
59. Broude,E.V., Swift,M.E., Vivo,C., Chang,B.-D., Davis,B.M., Kalurupalle,S., Blagosklonny,M.V. and Roninson,I.B. (2007) p21(Waf1/Cip1/Sdi1) mediates retinoblastoma protein degradation. *Oncogene*, **26**, 6954–6958.
60. Uchida,C., Miwa,S., Kitagawa,K., Hattori,T., Isobe,T., Otani,S., Oda,T., Sugimura,H., Kamijo,T., Ookawa,K. *et al.* (2005) Enhanced Mdm2 activity inhibits pRB function via ubiquitin-dependent degradation. *EMBO J.*, **24**, 160–169.
61. Liu,B., Yi,J., Yang,X., Liu,L., Lou,X., Zhang,Z., Qi,H., Wang,Z., Zou,J., Zhu,W.-G. *et al.* (2019) MDM2-mediated degradation of WRN promotes cellular senescence in a p53-independent manner. *Oncogene*, **38**, 2501–2515.
62. Lin,D., Fiscella,M., O'Connor,P.M., Jackman,J., Chen,M., Luo,L.L., Sala,A., Travali,S., Appella,E. and Mercer,W.E. (1994) Constitutive expression of B-myb can bypass p53-induced Waf1/Cip1-mediated G1 arrest. *Proc. Natl. Acad. Sci. U.S.A.*, **91**, 10079–10083.
63. Vassilev,L.T., Vu,B.T., Graves,B., Carvajal,D., Podlaski,F., Filipovic,Z., Kong,N., Kammlott,U., Lukacs,C., Klein,C. *et al.* (2004) In vivo activation of the p53 pathway by small-molecule antagonists of MDM2. *Science*, **303**, 844–848.
64. Tacar,O., Sriamornsak,P. and Dass,C.R. (2013) Doxorubicin: an update on anticancer molecular action, toxicity and novel drug delivery systems. *J. Pharm. Pharmacol.*, **65**, 157–170.
65. Matsuoka,S., Huang,M. and Elledge,S.J. (1998) Linkage of ATM to cell cycle regulation by the Chk2 protein kinase. *Science*, **282**, 1893–1897.
66. Harrington,E.A., Bruce,J.L., Harlow,E. and Dyson,N. (1998) pRB plays an essential role in cell cycle arrest induced by DNA damage. *Proc. Natl. Acad. Sci. U.S.A.*, **95**, 11945–11950.
67. Ji,P., Jiang,H., Rekhtman,K., Bloom,J., Ichetovkin,M., Pagano,M. and Zhu,L. (2004) An Rb-Skp2-p27 pathway mediates acute cell cycle inhibition by Rb and is retained in a partial-penetrance Rb mutant. *Mol. Cell*, **16**, 47–58.
68. Binné,U.K., Classon,M.K., Dick,F.A., Wei,W., Rape,M., Kaelin,W.G., Näär,A.M. and Dyson,N.J. (2007) Retinoblastoma protein and anaphase-promoting complex physically interact and functionally cooperate during cell-cycle exit. *Nat. Cell Biol.*, **9**, 225–232.
69. Talluri,S. and Dick,F.A. (2012) Regulation of transcription and chromatin structure by pRB: here, there and everywhere. *Cell Cycle*, **11**, 3189–3198.
70. Stewart-Ornstein,J. and Lahav,G. (2016) Dynamics of CDKN1A in single cells defined by an endogenous fluorescent tagging toolkit. *Cell Rep.*, **14**, 1800–1811.